Composite Structures 280 (2022) 114859

Contents lists available at ScienceDirect

Composite Structures

journal homepage: www.elsevier.com/locate/compstruct

The in-plane mechanics of a family of curved 2D lattices

S. Mukherjee [a], S. Adhikari [b,*]

[a] College of Engineering, Swansea University, Bay Campus, Swansea SA1 8EN, UK
[b] James Watt School of Engineering, The University of Glasgow, Glasgow G12 8QQ, UK

ARTICLE INFO

Keywords:
Elastic properties
Curved beams
Lattice materials
Mechanical metamaterials
Analytical mechanics

ABSTRACT

We propose an analytical framework to understand the mechanics and quantify the essential elastic properties of two-dimensional hexagonal lattices with curved elements. Generalised closed-form expressions for the in-plane Young's moduli and Poisson's ratios are obtained. It is of utmost importance to develop physics-based efficient computational models for the design and analysis of cellular metamaterials. This paper develops fundamental analytical approaches for obtaining generalised expressions to capture a large class of geometry. The closed-form expressions are obtained utilising the stiffness coefficients of the constituent structural members of the unit cell with curved beams. The new expressions for the equivalent in-plane properties are then explored to investigate seven other unique unit cell geometries including two auxetic configurations. Curved beam element as a constituent member of the unit cell has a significant effect in increasing the flexibility of the lattice and it also expands the design space for lattice materials. The Poisson's ratios also vary in a controlled way and this favourable feature can be exploited for obtaining designer values for both the regular and auxetic cases. The proposed analytical approach and the new closed-form expressions provide a computationally efficient and physically intuitive framework for the analysis and parametric design of curved lattice materials. The equivalent in-plane properties can be utilised as per the design requirements and the expressions can be considered as benchmark results for future numerical and experimental investigations.

1. Introduction

Mechanical metamaterials are architectured materials comprised of different length scales and developed by arranging unique micro-structures to achieve unprecedented macro-scale properties which are not available in nature [1–3]. Lattices are typical mechanical metamaterials which are formed by tessellating a periodic unit cell. The micro-structures effectively dictate the overall properties of the lattice. Due to the advancement of additive manufacturing, the research on lattice materials has increased substantially in recent times and researchers are exploring different metamaterials to obtain tailored properties. These artificially manufactured lattices are adopted from nature and hexagonal lattices have been studied extensively in different fields as they deliver high stiffness, toughness, and energy absorption properties. To understand the concept of cellular materials we refer to the work of Gibson and Ashby [4] and Fleck et al. [5]. Most of the researches are focused on obtaining higher stiffness to weight ratio for engineering applications and deals with straight constituent structural members. Whereas, depending on the application of the structure, flexibility is also an important objective to obtain the desired deformation. In this work, we explore the flexibility of lattice material considering curved constituent members for the unit cell of the lattice and proposed a novel class of 2D structural metamaterials.

The mechanical properties of the micro-architectured materials are dependent on the material and geometric properties of the constituent member of a periodic unit cell. In nature, we can find some materials with unintuitive material properties [5,6]. The recent advancement of additive manufacturing has opened a window to develop mechanical and structural metamaterials with unprecedented mechanical properties and structural qualities. Cutting-edge researches have been performed and are still being persuaded to obtain a novel class of metamaterials with user-defined properties. The geometric properties of constituent elements dictate the overall behaviour of the lattices and consequently, this opens up a significant opportunity to explore a wide range of geometric designs. The unit cell approach is a well known and widely used approach to obtain the equivalent material behaviour of the whole lattice [7–9]. It is mainly the honeycomb material that is being studied extensively [10–15] and utilised to manufacture structural members in the aerospace industry due to its high specific stiffness low relative density. Several studies are available in literature based on hexagonal lattice materials to predict the equivalent

* Corresponding author.
E-mail addresses: shuvajit.mukherjee@swansea.ac.uk (S. Mukherjee), Sondipon.Adhikari@glasgow.ac.uk (S. Adhikari).

https://doi.org/10.1016/j.compstruct.2021.114859
Received 11 June 2021; Received in revised form 14 October 2021; Accepted 17 October 2021
Available online 3 November 2021

elastic moduli for regular as well as irregular hexagonal lattice [16–21]. The metamaterials studied are with straight constituent elements and the main objective has been to increase the stiffness of the structure [22,23]. Although high stiffness is desirable in many applications, flexibility is also an important factor to satisfy the design requirements for morphing structure which has become an important field of research in the aerospace industry [24,25]. Flexibility is also crucial for a wide range of engineering applications such as bio-engineering, stretchable electronics, impact absorption and soft robots [26–31].

In this paper, we focus on hexagonal lattices with curved constitutive elements. Some examples of curved 2D lattices conceived and analysed in this paper are shown in Fig. 1. Four types of lattices depicted are (a) the curved hexagonal lattice, (b) the curved hexagonal auxetic lattice, (c) the curved rhombus lattice, and (d) the curved rectangular lattice. Although these lattices are physically very different, it will be shown that their mechanical behaviour can be quantified using a unified analytical formulation. Current works on 2D lattices are dominated by straight beam-element members to explore the behaviour of regular as well as auxetic hexagonal lattices [32,33]. With the straight structural members, the design space of modifying the equivalent Young's moduli and Poisson's ratio is limited. One way this limitation is addressed here is by modifying the conventional hexagonal geometry considering curved beam elements instead of straight ones. Following this direction, we proposed a comprehensive analytical approach that utilises the stiffness coefficients of the curved member elements to obtain the closed-form expressions for the equivalent material parameters. The formulation is performed for curved 2D lattices. Curved structures are of great importance in different engineering fields. Researchers explored the statics and dynamics of the curved beam through the decades [34–37]. Several research papers can be found on the development of finite element models of curved beam [38–41] considering various types of displacement functions [42,43]. Yamada and Ezawa [44] proposed an exact stiffness matrix formulation for the curved beam. Tufekci et al. [45] derived a two-noded curved beam finite element based on the exact solution of the differential equation of the curved beam considering axial and shear deformation. Lattice with curved geometry is used in literature to obtain soft metamaterials for highly stretchable applications [46–49]. In these works, the authors obtained the expressions for the material parameters using Castigliano's method. Curved beam is used in this work for the fact that it increases the flexibility of the element and also, we can have a broad design space to tune the equivalent Young's modulus and Poisson's ratio by varying the curvature angle along with the cell angle, length, thickness and other geometric parameters. For the case of straight beam element lattices, we do not have the option of varying the curvature angle. Therefore, we cannot obtain different material parameters by tuning the curvature angle. Depending on the design demand we can have different material properties and the limits of the material parameters are the ones with curvature angle zero i.e the regular conventional hexagonal lattice. This is a key reason behind exploring curved elements as a constituent member of the hexagonal lattice.

We propose a method to derive closed-form expressions for the in-plane elastic properties of the novel curved 2D lattice by exploiting the stiffness components of the constituent members. These expressions are general as one can obtain other geometries and conventional lattices directly from them as special cases. Analysis for both regular and auxetic lattices are performed and the flexibility of the structures are studied in great details. In the analysis, we also considered the axial stretching contributions of the constituent elements along with bending. We can see that the design space for this formulation is higher and one can tune the properties based on their requirements. The formulation of the closed-form expression is also simple and straight-forward where the stiffness coefficients of the stiffness matrix of the constituent members of the unit cell are directly utilised.

The paper is organised as follows. In Section 2, the unit cell approach is discussed and the stiffness matrices corresponding to the constituent beam elements are also mentioned in detail. The equivalent elastic properties for curved hexagonal lattice is derived in Section 3. The numerical results for the curved hexagonal lattice are obtained and discussed in Section 5. The Exact closed-form expressions for the equivalent elastic properties of different geometries and special cases are investigated which include auxetic curved hexagonal lattices, curved rhombus-shaped lattices, curved rectangular lattices, regular hexagonal lattice, auxetic hexagonal lattice and rectangular lattice in Section 6. The results corresponding to the different cases and their comparisons are discussed in Section 7 Finally, in Section 8 conclusions are drawn based on the present work.

2. Overview of the unit cell approach for equivalent elastic moduli

2.1. The unit cell model

The equivalent elastic property of a lattice material can be obtained by considering a suitable periodic unit cell. For a two-dimensional periodic lattice, the equivalent elastic properties are independent of the choice of the unit cell as long as it tessellates and physically represents the entire lattice. Therefore, to simplify the analysis it is customary to choose a unit cell. In Fig. 2 we show a representative example of a hexagonal curved lattice and its corresponding unit cell. Each of the cell walls bends and stretches when subjected to in-plane stress. When the applied stress is uniform along with the out of the plane, each element of the unit cell (Fig. 2) can be modelled as a beam. We can see that there are two types of beam components: 1. Curved beam and 2. straight beam. In the next subsection, we will briefly discuss the finite element analysis of these types of beams.

The equivalent elastic properties of a lattice material are important for global stress–strain analysis. In this work, we are concerned about the longitudinal Young's modulus E_1, the transverse Young's modulus E_2, and the Poisson's ratios ν_{12} and ν_{21}. There are two broad analytical approaches to obtain these equivalent elastic properties. The first is the direct force displacement-based method, pioneered by Gibson and Ashby [4]. The second approach is based on the stiffness coefficients of the constituent members of the unit cell [20]. Both approaches give identical results. However, the method based on stiffness coefficients is more general as it uses a finite element based approach. If the stiffness matrix of the constituent members can be obtained exactly, the equivalent elastic properties of the lattice can be expressed by exact closed-form expressions [21]. For this reason, we adopted the stiffness matrix based formulation considering the underlying physics of the constituent members.

Considering only the bending deformation and ignoring any stretching/shortening deformations, the equivalent elastic moduli of hexagonal cellular materials with straight beams are obtained by Gibson and Ashby [4] as

$$E_{1_{GA}} = E\alpha^3 \frac{\cos\theta}{(\eta+\sin\theta)} \frac{1}{\sin^2\theta} \tag{1}$$

$$E_{2_{GA}} = E\alpha^3 \frac{(\eta+\sin\theta)}{\cos^3\theta} \tag{2}$$

$$\nu_{12_{GA}} = \frac{\cos^2\theta}{(\eta+\sin\theta)\sin\theta} \tag{3}$$

and $$\nu_{21_{GA}} = \frac{(\eta+\sin\theta)\sin\theta}{\cos^2\theta} \tag{4}$$

In the above equations, the non-dimensional thickness ratio and the non-dimensional height ratio are given by

$$\alpha = \frac{t}{L} \tag{5}$$

and $$\eta = \frac{h}{L} \tag{6}$$

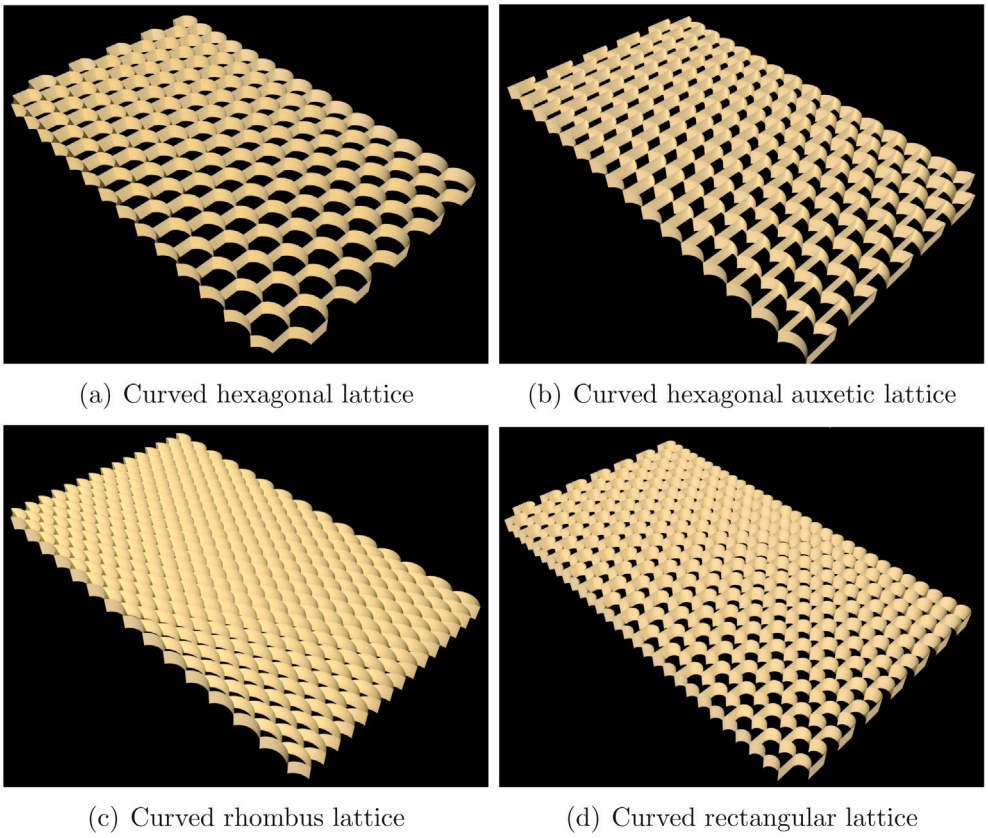

Fig. 1. Family of curved 2D lattices conceived and analysed in this paper (a) The curved hexagonal lattice, (b) The curved hexagonal auxetic lattice, (c) The curved rhombus lattice, and (d) The curved rectangular lattice.

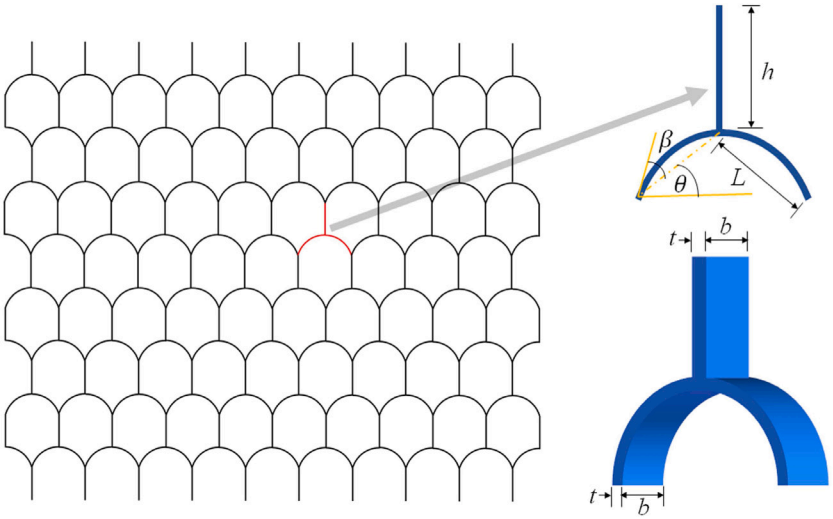

Fig. 2. Typical representation of a hexagonal curved lattice, unit cell and its 3D view. h=height of the straight beam element; L= Length of the curved beam element; β= Curvature angle; θ= Cell angle; b= width of the unit cell; t= thickness of the unit cell.

respectively. Here we are focused on the behaviour of the material in the primary directions and we obtained the closed-form expression of Young's moduli and Poisson's ratios for lattices with curved elements. The aim is to generalise Gibson and Ashby's expressions to the case of curved lattices.

2.2. The classical straight beam element

For the straight beam, we consider the Euler–Bernoulli beam element. The beam element with length L and three degrees of freedom (dof) per node is shown in Fig. 3(a). Considering the Euler–Bernoulli beam theory (see for example [50]), the governing equations for the transverse and axial deformations are given by

$$EI\frac{\partial^4 w}{\partial x^4} = f_b \tag{7}$$

and

$$EA\frac{\partial^2 u}{\partial x^2} = f_a \tag{8}$$

Here $w \equiv w(x)$ and $f_b \equiv f_b(x)$ denote the transverse displacement and applied transverse forcing on the beam and $u \equiv u(x)$ and $f_x \equiv$

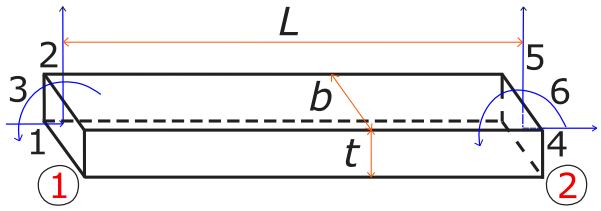

(a) Straight beam element

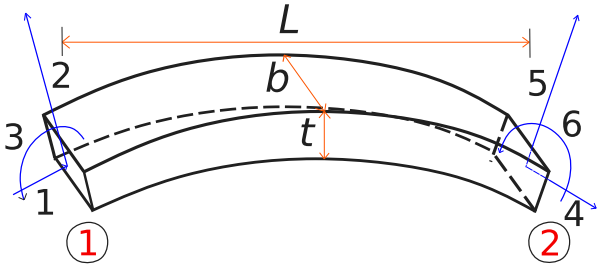

(b) Curved beam element

Fig. 3. Schematic diagram of a straight and curved beam element with three degrees of freedom (axial, transverse and rotational) per node. In the above figures b= width and t= thickness of the beam elements.

$f_a(x)$ represent the axial displacement and applied axial forcing on the beam. E is Young's modulus A is the cross sectional area of the beam and I is the moment of inertia moment of the beam cross section. Exact representation for the force–displacement relationship of beam equations (Eqs. (7) and (8)) can be done using finite element formulation considering cubic shape function for the bending and linear shape function for the axial deformation.

In general the six-degree-of-freedom (DOF) stiffness matrix of a beam comprising axial deformation, transverse deformation and rotation can be expressed [50,51] as

$$\mathbf{K} = \begin{bmatrix} \mathbf{K}_{11} & \mathbf{K}_{12} \\ \mathbf{K}_{21} & \mathbf{K}_{22} \end{bmatrix} \tag{9}$$

where $\mathbf{K}_{ij}, i, j = 1, 2$ are 3×3 sub-matrices. The degrees of freedom for the beam element are shown in Fig. 3(a). The complete stiffness matrix of the beam is given in closed-form as

$$\mathbf{K} = \begin{bmatrix} \frac{EA}{L} & 0 & 0 & -\frac{EA}{L} & 0 & 0 \\ 0 & \frac{12EI}{L^3} & \frac{6EI}{L^2} & 0 & -\frac{12EI}{L^3} & \frac{6EI}{L^2} \\ 0 & \frac{6EI}{L^2} & \frac{4EI}{L} & 0 & -\frac{6EI}{L^2} & \frac{2EI}{L} \\ -\frac{EA}{L} & 0 & 0 & \frac{EA}{L} & 0 & 0 \\ 0 & -\frac{12EI}{L^3} & -\frac{6EI}{L^2} & 0 & \frac{12EI}{L^3} & -\frac{6EI}{L^2} \\ 0 & \frac{6EI}{L^2} & \frac{2EI}{L} & 0 & -\frac{6EI}{L^2} & \frac{4EI}{L} \end{bmatrix} \tag{10}$$

The degrees of freedom 1 and 4 correspond to the axial displacements, degrees of freedom 2 and 5 denotes the transverse displacements, and 3 and 6 correspond to the rotations of the cross sections.

2.3. The curved beam element

To model the curved beam, we have considered the exact stiffness matrix formulation by Yamada and Ezawa [44]. Their formulation account for the axial stretching along with the bending deformation. Fig. 3(b) shows the schematic of the two noded curved beam element with 3 degrees of freedom per node. Fig. 4 shows the curved beam under equilibrium forces. The equilibrium equations considering a section on the curved beam are as follows

$$N + N_C \cos\phi - Q_C \sin\phi = 0 \tag{11}$$

$$Q + N_C \sin\phi + Q_C \cos\phi = 0 \tag{12}$$

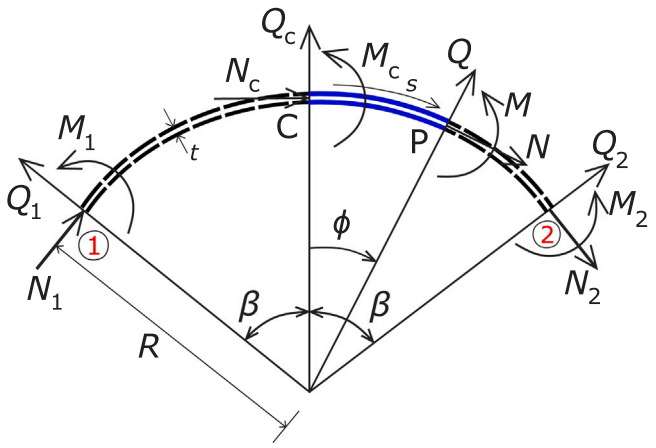

Fig. 4. Schematic diagram of a curved beam element in equilibrium. N, M and Q denote the axial force, moment and shear force respectively.

$$\text{and} \quad M + M_C - N_C R(1 - \cos\phi) - Q_C R \sin\phi = 0 \tag{13}$$

Where N, M and Q are the axial, moment and shear forces respectively. The central section is denoted by subscript C and R is the radius. Angle β denotes the curvature angle and ϕ is the variable angle that specifies the position of point P on the beam. The strain and the rotation are given by

$$\varepsilon = \mathrm{d}u_t/\mathrm{d}s + u_r/R \tag{14}$$

$$\text{and} \quad \delta\phi = \mathrm{d}u_r/\mathrm{d}s - u_t/R \tag{15}$$

where $s = R\phi$ in Fig. 4 denotes the arch length. The quantities u_t and u_r are the tangential and radial displacements respectively. The curvature is expressed as

$$\kappa = \frac{\mathrm{d}\delta\phi}{\mathrm{d}s} = \frac{1}{R^2}\left(\frac{\mathrm{d}^2 u_r}{\mathrm{d}\phi^2} - \frac{\mathrm{d}u_t}{\mathrm{d}\phi}\right) \tag{16}$$

For elastic beam, the constitutive equations are as follows

$$\varepsilon = N/EA \tag{17}$$

$$\text{and} \quad \kappa = \mathrm{d}\delta\phi/\mathrm{d}s = M/EI \tag{18}$$

where EI and EA are the bending stiffness and axial stiffness of the beam respectively. I and A are the moment of inertia and area of the cross-section of the beam. E denote Young's modulus of the beam material. Considering the above equations we obtain the governing equations for the tangential and radial displacements as

$$\frac{1}{R}\left(\frac{\mathrm{d}u_t}{\mathrm{d}\phi} + u_r\right) = \frac{1}{EA}\left(Q_C \sin\phi - N_C \cos\phi\right) \tag{19}$$

and

$$\frac{1}{R^2}\left(\frac{\mathrm{d}^2 u_r}{\mathrm{d}\phi^2} - \frac{\mathrm{d}u_t}{\mathrm{d}\phi}\right) = \frac{1}{EI}\left[-M_C + N_C R(1 - \cos\phi) + Q_C R \sin\phi\right] \tag{20}$$

Eqs. (19) and (20) are equivalent to the case of the straight beams in Eq. (8) and Eq. (7) respectively. However, there is a distinct difference between those equivalent equations. Unlike the straight beam equation the curved beam equations are coupled. These two equations (Eqs. (19) and (20)) are then used to obtain the tangential and radial displacements followed by the flexibility and stiffness matrix for curved beam. For further details we refer to [44].

Like the straight beam element, the curved beam element also has six degrees of freedom. Therefore, the stiffness matrix of the curved beam can be expressed in a manner similar to the straight beam given in Eq. (9). While the physical meaning of the individual elements of the stiffness matrix remains the same, the expressions themselves are more complex. The exact closed-form expressions of the 3×3 sub-matrices, $\mathbf{K}_{ij}, i, j = 1, 2$ are given in Boxes I–III.

$$\mathbf{K}_{11} = D\begin{bmatrix} \beta^2-\beta\left(\cos^2\beta-\sin^2\beta\right)\sin\beta\cos\beta & & Sym. \\ \quad -\frac{2}{1+\xi}\sin^4\beta & & \\ 2\beta\sin^2\beta\cos^2\beta & \beta^2+\beta\left(\cos^2\beta-\sin^2\beta\right)\sin\beta\cos\beta & \\ \quad -\frac{2}{1+\xi}\sin^3\beta\cos\beta & \quad -\frac{2}{1+\xi}\sin^2\beta\cos^2\beta & \\ \beta^2-2\beta\cos^3\beta\sin\beta & \beta(1+2\cos^2\beta)\sin^2\beta & \beta^2\left[1+\frac{1}{2}(1+\xi)\right] \\ \quad +\left(\cos^2\beta-\frac{2}{1+\xi}\sin^2\beta\right)\sin^2\beta & \quad -\left(\frac{2}{1+\xi}+1\right)\sin^3\beta\cos\beta & \quad -\beta(1+2\cos^2\beta)\sin\beta\cos\beta \\ & & \quad +\left\{\left[2-\frac{1}{2}(1+\xi)\right]\cos^2\beta\right. \\ & & \quad \left.-\frac{2}{1+\xi}\sin^2\beta\right\}\sin^2\beta \end{bmatrix} \tag{21}$$

Box I.

$$\mathbf{K}_{12} = D\begin{bmatrix} \beta^2\left(\sin^2\beta-\cos^2\beta\right) & -2\beta^2\sin\beta\cos\beta & \beta^2\left(\sin^2\beta-\cos^2\beta\right) \\ \quad +\beta\sin\beta\cos\beta & \quad +\frac{2}{1+\xi}\sin^3\beta\cos\beta & \quad +2\beta\sin\beta\cos\beta \\ \quad -\frac{2}{1+\xi}\sin^4\beta & & \quad -\left(\cos^2\beta+\frac{2}{1+\xi}\sin^2\beta\right)\sin^2\beta \\ 2\beta^2\sin\beta\cos\beta & \beta^2\left(\sin^2\beta-\cos^2\beta\right) & 2\beta^2\sin\beta\cos\beta \\ \quad -\frac{2}{1+\xi}\sin^3\beta\cos\beta & \quad -\beta\sin\beta\cos\beta & \quad -\beta\sin^2\beta \\ & \quad +\frac{2}{1+\xi}\sin^2\beta\cos^2\beta & \quad -\left(\frac{2}{1+\xi}-1\right)\sin^3\beta\cos\beta \\ \beta^2\left(\sin^2\beta-\cos^2\beta\right) & -2\beta^2\sin\beta\cos\beta & \beta^2\left[\sin^2\beta-\cos^2\beta-\frac{1}{2}(1+\xi)\right] \\ \quad +2\beta\sin\beta\cos\beta & \quad +\beta\sin^2\beta & \quad +3\beta\sin\beta\cos\beta \\ \quad -\left(\cos^2\beta+\frac{2}{1+\xi}\sin^2\beta\right)\sin^2\beta & \quad +\left(\frac{2}{1+\xi}-1\right)\sin^3\beta\cos\beta & \quad -\left\{\left[2-\frac{1}{2}(1+\xi)\right]\cos^2\beta\right. \\ & & \quad \left.+\frac{2}{1+\xi}\sin^2\beta\right\}\sin^2\beta \end{bmatrix} = \mathbf{K}_{21}^T \tag{22}$$

Box II.

$$\mathbf{K}_{22} = D\begin{bmatrix} \beta^2-\beta\left(\cos^2\beta-\sin^2\beta\right)\sin\beta\cos\beta & & Sym \\ \quad -\frac{2}{1+\xi}\sin^4\beta & & \\ -2\beta\sin^2\beta\cos^2\beta & \beta^2+\beta\left(\cos^2\beta-\sin^2\beta\right)\sin\beta\cos\beta & \\ \quad +\frac{2}{1+\xi}\sin^3\beta\cos\beta & \quad -\frac{2}{1+\xi}\sin^2\beta\cos^2\beta & \\ \beta^2-2\beta\cos^3\beta\sin\beta & -\beta(1+2\cos^2\beta)\sin^2\beta & \beta^2\left[1+\frac{1}{2}(1+\xi)\right] \\ \quad +\left(\cos^2\beta-\frac{2}{1+\xi}\sin^2\beta\right)\sin^2\beta & \quad +\left(\frac{2}{1+\xi}+1\right)\sin^3\beta\cos\beta & \quad -\beta(1+2\cos^2\beta)\sin\beta\cos\beta \\ & & \quad +\left\{\left[2-\frac{1}{2}(1+\xi)\right]\cos^2\beta\right. \\ & & \quad \left.-\frac{2}{1+\xi}\sin^2\beta\right\}\sin^2\beta \end{bmatrix} \tag{23}$$

Box III.

In the above matrix equations

$$D = \frac{EI}{R^3}\bar{D} = \frac{EI/R^3}{(1+\xi)\beta\left(\beta^2-\sin^2\beta\cos^2\beta\right)-2(\beta-\sin\beta\cos\beta)\sin^2\beta} \tag{24}$$

and the non-dimensional quantities

$$\bar{D} = \frac{1}{(1+\xi)\beta\left(\beta^2-\sin^2\beta\cos^2\beta\right)-2(\beta-\sin\beta\cos\beta)\sin^2\beta} \tag{25}$$

and

$$\xi = \frac{I}{AR^2} = \frac{1}{12}\frac{bt^3}{(bt)R^2} = \frac{1}{12}\left(\frac{t}{R}\right)^2 = \frac{1}{3}\alpha^2\sin^2\beta \tag{26}$$

The preceding relationship arises from the fact that $R = L/(2\sin\beta)$ (see Fig. 5 for the geometric details). In this work, it turns out that the stiffness coefficients within the block $\mathbf{K}_{11}$ are mainly necessary for further derivation. They are represented as below for convenience

$$\mathbf{K}_{11} = D\begin{bmatrix} k_{11} & k_{12} & k_{13} \\ k_{12} & k_{22} & k_{23} \\ k_{13} & k_{23} & k_{33} \end{bmatrix} = \frac{EI}{R^3}\bar{D}\begin{bmatrix} k_{11} & k_{12} & k_{13} \\ k_{12} & k_{22} & k_{23} \\ k_{13} & k_{23} & k_{33} \end{bmatrix} = \frac{2}{3}Eb\alpha^3\bar{D}\sin^3\beta\begin{bmatrix} k_{11} & k_{12} & k_{13} \\ k_{12} & k_{22} & k_{23} \\ k_{13} & k_{23} & k_{33} \end{bmatrix}$$

$$= \frac{2}{3}Eb\alpha^3 \begin{bmatrix} \bar{k}_{11} & \bar{k}_{12} & \bar{k}_{13} \\ \bar{k}_{12} & \bar{k}_{22} & \bar{k}_{23} \\ \bar{k}_{13} & \bar{k}_{23} & \bar{k}_{33} \end{bmatrix} = D_L \begin{bmatrix} \bar{k}_{11} & \bar{k}_{12} & \bar{k}_{13} \\ \bar{k}_{12} & \bar{k}_{22} & \bar{k}_{23} \\ \bar{k}_{13} & \bar{k}_{23} & \bar{k}_{33} \end{bmatrix} \tag{27}$$

where $D_L = \frac{2}{3}Eb\alpha^3$. It can be seen that the components of $\mathbf{K}_{11}$ are functions of the curvature angle β. If we take the $\lim_{\beta\to 0}$ of $\mathbf{K}_{11}$ it becomes the stiffness components of the Euler–Bernoulli beam as shown below

$$\lim_{\beta\to 0}\mathbf{K}_{11} = \lim_{\beta\to 0} D \begin{bmatrix} k_{11} & k_{12} & k_{13} \\ k_{12} & k_{22} & k_{23} \\ k_{13} & k_{23} & k_{33} \end{bmatrix} = \begin{bmatrix} k_{11}^{EB} & k_{12}^{EB} & k_{13}^{EB} \\ k_{12}^{EB} & k_{22}^{EB} & k_{23}^{EB} \\ k_{13}^{EB} & k_{23}^{EB} & k_{33}^{EB} \end{bmatrix}$$
$$= \begin{bmatrix} \frac{EA}{L} & 0 & 0 \\ 0 & \frac{12EI}{L^3} & \frac{6EI}{L^2} \\ 0 & \frac{6EI}{L^2} & \frac{4EI}{L} \end{bmatrix} \tag{28}$$

The components of the stiffness matrix from Eq. (27) and Eq. are used in next section to derive the equivalent elastic coefficients of the general curved 2D lattice.

3. The general derivation of in-plane elastic moduli

The elastic behaviour of the overall lattice material depends on the deformation characteristics of the constituent individual beams. In the previous section, the stiffness matrices of a curved beam and a straight beam element are discussed. The objective of this section is to express equivalent in-plane elastic moduli of the lattice in terms of the stiffness matrix elements of the curved beams using the unit cell approach. For the case of equivalent static properties of the straight-beam lattices, we refer to well-known references by Gibson and Ashby [4] and Masters and Evans [7]. For the sake of generality, we consider the equilibrium of the unit cell under different stress conditions.

3.1. The longitudinal Young's modulus E_1 and the Poisson's ratio ν_{12}

To obtain the expression of longitudinal elastic modulus, uniform stress is applied to the unit cell in the 1-direction. The boundary conditions of the unit cell are chosen in such a way that it can capture the physics of the hexagonal lattice material under in-plane loading conditions. The main motivation is to utilise the stiffness components of the constituent beam members directly into the formulation to obtain the equivalent material properties of the lattice. The employment of the stiffness matrix coefficients ensures that the forces and moments arising from the deformations of the adjacent cells due to the application of the global stress fields are taken into account in a mechanically consistent manner. This is equivalent to the direct force method considered by Gibson and Ashby [4] and Masters and Evans [7].

Therefore, we choose a single cell and the equivalent material properties are obtained by prescribing appropriate boundary conditions. The entire lattice is formed by tessellating the unit cell in the x and y directions. The boundary conditions imposed are as follows:

- Point C is fixed.
- The rotational degrees of freedom are restrained in points A and B.

The deformation of the unit cell is symmetric about the member OC. The resultant force P is the consequence of the applied stress which is acting on points A and B of the unit cell (Fig. 5). The effect of rotation of the adjacent cells at points A and B will be equal and opposite and therefore, in this unit cell, the rotational dof are constrained. At point O, there will also act equal and opposite forces and moments and consequently there will be no net deformation of the point. Also, the vertical member will not experience any displacements, so the point C is kept fixed. These boundary conditions along with the above deformation patterns ensure the periodicity of the unit cell when the overall deformation of the entire lattice is considered in both directions.

The expression of the force P is obtained by multiplying the stress with the effective area as

$$P = \sigma_1 b(h + L\sin\theta) \tag{29}$$

The components of P in the tangential and radial direction of the curved beam are respectively $P_t = P\cos\theta$ and $P_r = P\sin\theta$. The local coordinate systems for a curved beam, as well as for the unit cell, are shown in Fig. 6.

Now, considering the force–displacement relationship of a curved beam we get

$$P_t = k_{11}u_t + k_{12}u_r \tag{30}$$
$$\text{and} \quad P_r = k_{21}u_t + k_{22}u_r \tag{31}$$

Here the terms $k_{ij}(i,j=1,2)$ in the above equations are to be obtained from form Eq. (27) corresponding to the $\mathbf{K}_{11}$ block of the overall stiffness matrix. Solving the above equations the values of u_t and u_r can be obtained as

$$u_t = \frac{k_{22}P_t - k_{12}P_r}{k_{11}k_{22} - k_{12}^2} = \frac{k_{22}P_t - k_{12}P_r}{\Delta} \tag{32}$$
$$\text{and} \quad u_r = \frac{k_{11}P_r - k_{12}P_t}{k_{11}k_{22} - k_{12}^2} = \frac{k_{11}P_r - k_{12}P_t}{\Delta} \tag{33}$$

where

$$\Delta = k_{11}k_{22} - k_{12}^2 = D_L^2 \underbrace{\left[\bar{k}_{11}\bar{k}_{22} - \bar{k}_{12}^2\right]}_{\bar{\Delta}} = D_L^2\bar{\Delta} \tag{34}$$

$\bar{k}_{ij}$s are defined in Eq. (27). The displacements along the global co-ordinate system of the curved beam are

$$u_1' = u_t\cos\beta - u_r\sin\beta \tag{35}$$
$$\text{and} \quad u_2' = u_t\sin\beta + u_r\cos\beta \tag{36}$$

The displacements of point A with respect to the global co-ordinate system of the unit cell is

$$u_1 = u_1'\cos\theta - u_2'\sin\theta \tag{37}$$
$$\text{and} \quad u_2 = u_1'\sin\theta + u_2'\cos\theta \tag{38}$$

Putting the values of u_1' and u_2' in the above equations we obtain the expressions for the global displacements as

$$u_1 = u_t\cos(\beta+\theta) - u_r\sin(\beta+\theta) = u_t\cos\theta' - u_r\sin\theta' \tag{39}$$
$$\text{and} \quad u_2 = u_t\sin(\beta+\theta) + u_r\cos(\beta+\theta) = u_t\sin\theta' + u_r\cos\theta' \tag{40}$$

In the above equation it is considered that

$$\theta' = \theta + \beta \tag{41}$$

for notational convenience. Recalling that the unit cell is symmetric, the displacements at points A and B will be the same as the forcing is also symmetric. Therefore, the strain in the 1-direction can be obtained from the ratio of u_1 to the half-length of the unit cell as

$$\epsilon_1 = \frac{u_1}{L\cos\theta} = \frac{P}{\Delta L\cos\theta}\left[k_{11}\sin^2\theta' + k_{22}\cos^2\theta' + k_{12}\sin 2\theta'\right] \tag{42}$$

Using this, we obtain Young's modulus in 1-direction in terms of the elements of the stiffness matrix

$$E_1 = \frac{\sigma_1}{\epsilon_1} = \frac{\Delta\cos\theta}{b(\eta+\sin\theta)\left[k_{11}\sin^2\theta' + k_{22}\cos^2\theta' + k_{12}\sin\ 2\theta'\right]}$$
$$= \frac{D_L\bar{\Delta}\cos\theta}{b(\eta+\sin\theta)\left[\bar{k}_{11}\sin^2\theta' + \bar{k}_{22}\cos^2\theta' + \bar{k}_{12}\sin\ 2\theta'\right]}$$
$$= \frac{2}{3}E\alpha^3\frac{\bar{\Delta}\cos\theta}{(\eta+\sin\theta)\left[\bar{k}_{11}\sin^2\theta' + \bar{k}_{22}\cos^2\theta' + \bar{k}_{12}\sin\ 2\theta'\right]} \tag{43}$$

In the above, $\bar{k}_{ij}$s are mentioned in Eq. (27) and $\bar{\Delta}$ is defined in Eq. (34). The strain in the 2-direction is obtained as

$$\epsilon_2 = \frac{u_2}{h+L\sin\theta} = \frac{P}{\Delta}(k_{12}\cos 2\theta' + 0.5(k_{11}-k_{22})\sin 2\theta')$$

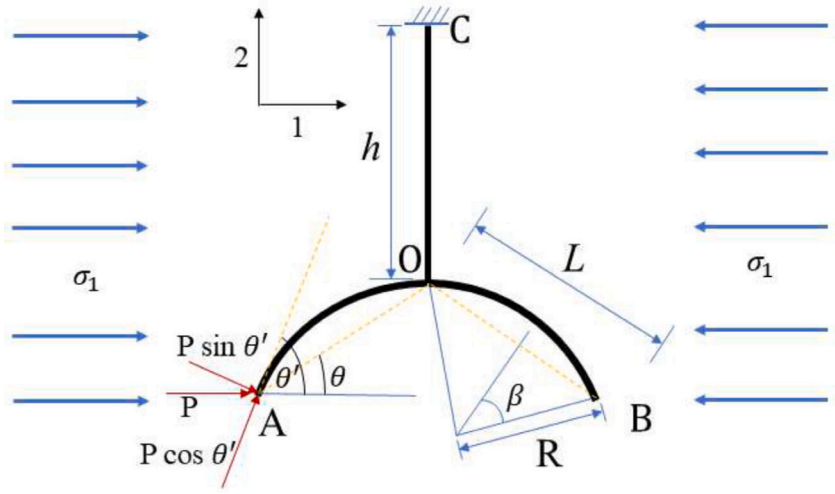

Fig. 5. The unit cell under the application of a stress field σ_1 is applied in the 1-direction. This configuration is used for the derivation of the longitudinal Young's modulus E_1 and the Poisson's ratio ν_{12}.

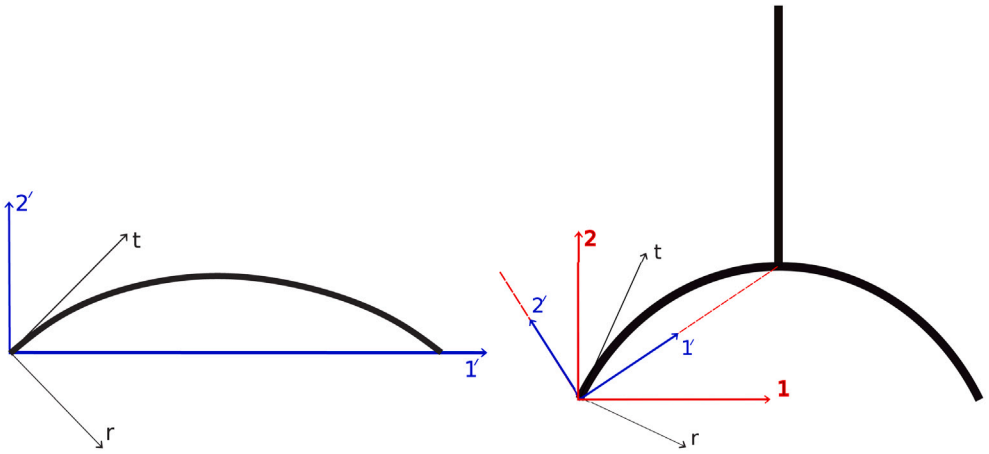

(a) co-ordinate system of a single curved beam (b) co-ordinate system of the unit cell

Fig. 6. The coordinate system of a curved beam and the unit cell. r and t denotes the radial and tangent co-ordinate of a curved beam; 1′ and 2′ denotes the global co-ordinate of a curved beam and 1 and 2 denotes the global co-ordinate system for the unit cell.

$$= \frac{\sigma_1 b}{\Delta}(k_{12}\cos 2\theta' + 0.5(k_{11} - k_{22})\sin 2\theta') \tag{44}$$

Using the strains ϵ_2 and ϵ_1, it is now possible to obtain the Poisson's ratio ν_{12} as

$$\nu_{12} = -\frac{\epsilon_2}{\epsilon_1} = \frac{\cos\theta}{(\eta + \sin\theta)} \frac{\left[\bar{k}_{12}\cos 2\theta' + 0.5(\bar{k}_{11} - \bar{k}_{22})\sin 2\theta'\right]}{\left[\bar{k}_{11}\sin^2\theta' + \bar{k}_{22}\cos^2\theta' + \bar{k}_{12}\sin\ 2\theta'\right]} \tag{45}$$

From the expressions derived here, we can observe that not only the diagonal terms but also the coupling terms contribute towards the value of E_1 and ν_{12}. This shows that the effect of the bending and stretching and their coupling is going to influence the material properties. This is a striking difference from the case of lattices with straight beams only. We will see the impact of this coupling in the results and discussion sections later in the paper.

3.2. The transverse Young's modulus E_2 and the Poisson's ratio ν_{21}

We derive the expression of transverse Young's modulus (E_2) and Poisson's ratio (ν_{21}) considering an uniform stress σ_2 in the global direction 2 (see Fig. 7). The components of W in the tangential and radial direction of the curved beam are respectively $P_t = W\sin\theta$ and $P_r = W\cos\theta$. The deformation is symmetric about line OC and the point O has deflection only in 2-direction. Following the similar procedure in Section 3.1 the global displacements are obtained as

$$u_1 = u_t\cos(\beta+\theta) - u_r\sin(\beta+\theta) = u_t\cos\theta' - u_r\sin\theta' \tag{46}$$

$$\text{and} \quad u_2 = u_t\sin(\beta+\theta) + u_r\cos(\beta+\theta) = u_t\sin\theta' + u_r\cos\theta' \tag{47}$$

Putting the values of u_t and u_r in the above equation and performing some algebraic simplifications, the displacements are obtained followed by Young's modulus and Poisson's ratio. The strain the 1-direction is obtained as

$$\epsilon_1 = \frac{u_1}{L\cos\theta} = \frac{W}{\Delta L\cos\theta}(\bar{k}_{12}\cos 2\theta' + 0.5(\bar{k}_{11} - \bar{k}_{22})\sin 2\theta') \tag{48}$$

The total displacement along the 2-direction is

$$\delta_2 = u_2 + \delta_o = u_2 + \frac{2W}{\frac{EA}{h}} \tag{49}$$

Where u_2 is the displacement of point A relative to point O and δ_0 is the displacement of point O in the 2-direction due to the axial deformation

Table 1
Details of the geometric parameters of the unit cell and the entire lattice considered for the finite element analysis.

Length (mm)	Thickness (mm)	Width (mm)	L_x (mm)	L_y (mm)	Cell angle (θ)
$l = h = 20.866$	t=1.50	b=1.50	724.32	480.78	30^0

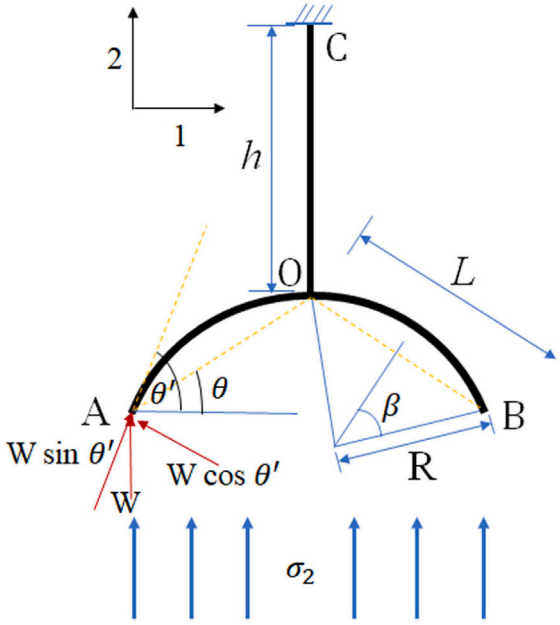

Fig. 7. The unit cell under the application of a stress field σ_2 is applied in the 2-direction. This configuration is used for the derivation of the longitudinal Young's modulus E_2 and the Poisson's ratio ν_{21}.

of the vertical member OC. The strain the 2-direction is therefore

$$\epsilon_2 = \frac{\delta_2}{h + L\sin\theta} = \frac{W}{\Delta}\frac{\left[(k_{11}\cos^2\theta' + k_{22}\sin^2\theta' - k_{12}\sin\ 2\theta') - \frac{2\Delta}{K^h_{44}}\right]}{(h + L\sin\theta)} \tag{50}$$

From the expression of the strain, Young's modulus for the 2-direction can be obtained as

$$\begin{aligned} E_2 &= \frac{\sigma_2}{\epsilon_2} = \frac{\Delta(\eta + \sin\theta)}{b\left[(k_{11}\cos^2\theta' + k_{22}\sin^2\theta' - k_{12}\sin\ 2\theta') - \frac{2\Delta}{K^h_{44}}\right]\cos\theta} \\ &= \frac{2}{3}E\alpha^3\frac{\bar{\Delta}(\eta + \sin\theta)}{\left[(\bar{k}_{11}\cos^2\theta' + \bar{k}_{22}\sin^2\theta' - \bar{k}_{12}\sin\ 2\theta') - \frac{4}{3}\eta\alpha^2\right]\cos\theta} \end{aligned} \tag{51}$$

In the above equation, K^h_{44} is the stiffness component of the vertical straight beam, $\bar{k}_{ij}$s are defined in Eq. (27) and $\bar{\Delta}$ is defined in Eq. (34). The Poisson's ratio is obtained in terms of the elements of the stiffness matrix as

$$\nu_{21} = -\frac{\epsilon_1}{\epsilon_2} = \frac{(\eta + \sin\theta)(\bar{k}_{12}\cos 2\theta' + 0.5(\bar{k}_{11} - \bar{k}_{22})\sin 2\theta')}{\left[(\bar{k}_{11}\cos^2\theta' + \bar{k}_{22}\sin^2\theta' - \bar{k}_{12}\sin\ 2\theta') - \frac{4}{3}\eta\alpha^2\right]\cos\theta} \tag{52}$$

The proposed expressions of the general equivalent material parameters conform the reciprocal theorem

$$\begin{aligned} E_1\nu_{21} = E_2\nu_{12} &= \frac{2}{3}E\alpha^3 \\ &\times \frac{\bar{\Delta}(\bar{k}_{12}\cos 2\theta' + 0.5(\bar{k}_{11} - \bar{k}_{22})\sin 2\theta')}{\left[\bar{k}_{11}\sin^2\theta' + \bar{k}_{22}\cos^2\theta' + \bar{k}_{12}\sin\ 2\theta'\right]\left[(\bar{k}_{11}\cos^2\theta' + \bar{k}_{22}\sin^2\theta' - \bar{k}_{12}\sin\ 2\theta') - \frac{4}{3}\eta\alpha^2\right]} \end{aligned} \tag{53}$$

The expressions derived here and in the previous subsection can be viewed as the generalisation of the classical results by Gibson and Ashby [4] for lattices with straight beam elements to lattices with curved beam elements. These analytical expressions actually converge to the formula obtained by Adhikari et al. [20] in the limiting case shown in Section 6.4 (Eqs. (76)–(79)). Also, Fig. 8 in Section 4 shows the convergence of the equivalent elastic properties to the Gibson and Ashby's expressions (Eqs. (1)–(4)) for small values of the curvature angle. This convergence verifies the closed-form expressions derived here.

Table 2
Elastic properties used for finite element simulation.

Material	Young's Modulus (GPa)	Poisson's ratio
Steel (ASTM-A36)	200	0.30

4. Validation of the closed-form solutions

4.1. Validation with respect to the classical analytical results

We first perform a comparison between our proposed closed-form expressions, Gibson and Ashby's expressions, and Masters and Evans solutions. Fig. 8 presents the values of E and ν for the regular and the auxetic case considering our formula, Gibson and Ashby's [4] formula and Masters and Evans's [7] formula. It is observed that for small values of β, our results converge to the Masters and Evans's formula.

The trend of the curves for Young's moduli is similar for both regular and auxetic cases. Whereas, the Poisson's ratio are opposite in sign as expected. The figure demonstrates that the expressions for the curved lattice are more general as the expressions for different geometry and classical cases can be obtained by limiting some parameters which already explained in Section 6.

4.2. Validation with respect to commercial finite element results

The finite element (FE) validation of the closed-form expressions for the regular hexagonal lattice with a straight constituent beam is also conducted in this section. Fig. 9(a) also shows the lattice material, boundary condition, and loading condition applied to the lattice to perform the finite element simulation. To perform the finite element analysis commercial software NASTRAN has been used. The unit cell of the lattice is shown in Fig. 12(e). The analytical expressions for the equivalent elastic moduli of regular hexagonal lattice are obtained in Section 6.4. For finite element validation we consider the longitudinal elastic modulus E_1 and to obtain the analytical value (76) is considered. The details of the geometric parameters of the unit cell and the whole lattice used for the finite element analysis are shown in Table 1. For material, Steel (ASTM-A36) is used for analysis. Elastic properties of these five materials are given in Table 2.

Solid elements with 1057332 nodes and 516475 elements are selected. The boundary conditions for the finite element model are considered in such a way that it can capture the deformation of the lattice as a 'material'. In this regard, the left faces of the lattice are allowed to move in the y-direction, but all other degrees of freedom are restricted. To avoid the rigid body displacements, the mid node is restricted to move in the y-direction, whereas all other degrees of freedom are released, which also supports the symmetry of the lattice structure. To obtain the equivalent longitudinal Young's modulus, the average displacements of all the nodes at the right edge of the lattice (where the load is applied). This average displacement is then divided

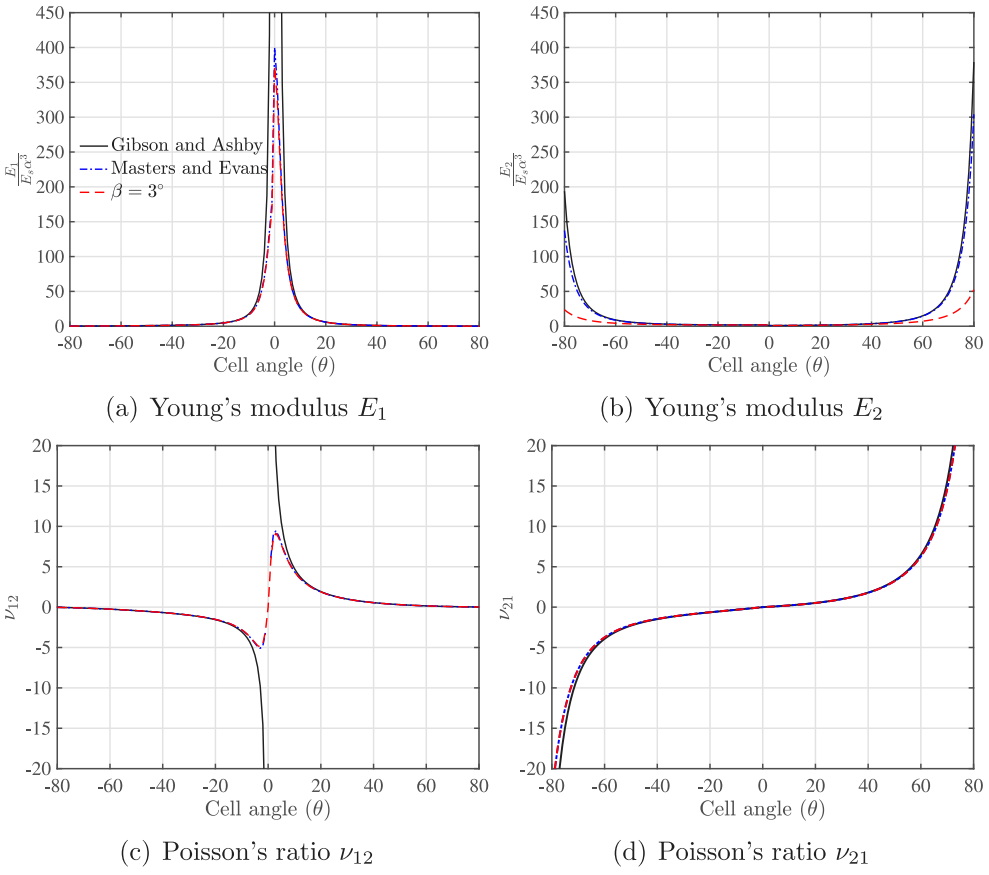

Fig. 8. Normalised equivalent elastic moduli and Poisson's ratio obtained for regular and auxetic case considering curved lattice (curvature angle $\beta = 3°$), Masters and Evans and Gibson and Ashby formula for cell angle $\theta < 0$, height ratio $\eta = \frac{h}{L} = 2$ and for cell angle $\theta \geq 0$, height ratio $\eta = \frac{h}{L} = 1$.

Table 3
Comparison of the normalised longitudinal Young's modulus ($E_1/(E\alpha^3)$) for the regular hexagonal lattices obtained from closed-form solution and finite element analysis. For E, the value of Young's modulus of Steel is considered.

Material	Analytical	FE	% error
Steel (ASTM-A36)	2.2741	2.2789	0.21

by the length of the lattice (L_x) to obtain the strain. The total force is divided with the surface area of the edge to derive the effective stress. Finally, to obtain the equivalent Young's modulus, the stress is divided with the effective strain. The typical deformation pattern of the lattice material under the application of a uniformly distributed load is shown in Fig. 9(b).

Table 3 shows the comparison between the analytical results are with finite element simulation. The value of $\alpha = t/l \approx 0.072$ in our analysis. The result shows a quite good match between the finite element and the analytical one.

5. Numerical results: curved hexagonal lattices

This section deals with the numerical analysis of the curved hexagonal lattice. The results are obtained by varying the curvature angle (β) and cell angle (θ) values. In Fig. 10 Young's modulus and Poisson's ratios are compared with the classical case.

For this plot, we kept the height ratio $\eta = 1$ and the material parameters are obtained as functions of the cell angle θ for different curvature angles (β). To analytically comprehend the difference between the classical results for straight lattices and curved lattices, we obtain the following explicit ratios

$$\frac{E_1}{E_{1_{GA}}} = \frac{2}{3}\frac{(\bar{k}_{11}\bar{k}_{22} - \bar{k}_{12}^2)}{\left[\bar{k}_{11}\sin^2\theta' + \bar{k}_{22}\cos^2\theta' + \bar{k}_{12}\sin\ 2\theta'\right]} \tag{54}$$

$$\frac{E_2}{E_{2_{GA}}} = \frac{2}{3}\frac{\cos^2\theta(\bar{k}_{11}\bar{k}_{22} - \bar{k}_{12}^2)}{\left[(\bar{k}_{11}\cos^2\theta' + \bar{k}_{22}\sin^2\theta' - \bar{k}_{12}\sin\ 2\theta') - \frac{4}{3}\eta\alpha^2\right]} \tag{55}$$

$$\frac{\nu_{12}}{\nu_{12_{GA}}} = \frac{\tan\theta\left(\bar{k}_{12}\cos 2\theta' + 0.5(\bar{k}_{11} - \bar{k}_{22})\sin 2\theta'\right)}{\left[\bar{k}_{11}\sin^2\theta' + \bar{k}_{22}\cos^2\theta' + \bar{k}_{12}\sin\ 2\theta'\right]} \tag{56}$$

$$\text{and} \quad \frac{\nu_{21}}{\nu_{21_{GA}}} = \frac{\cot\theta(\bar{k}_{12}\cos 2\theta' + 0.5(\bar{k}_{11} - \bar{k}_{22})\sin 2\theta')}{\left[(\bar{k}_{11}\cos^2\theta' + \bar{k}_{22}\sin^2\theta' - \bar{k}_{12}\sin\ 2\theta') - \frac{4}{3}\eta\alpha^2\right]} \tag{57}$$

In the special case of a straight lattice made of thin beam elements, that is, $\beta \to 0$ and $\alpha^2 \ll 1$, it can be proved that these four ratios become exactly 1. This implies that the ratios given in Eqs. (54)–(57) directly quantify the impact of curved lattices in relation to the straight lattices.

From Fig. 10 it is observed that the normalised values of E_1 and ν_{12} are quite less from the classical case for lower values of θ, whereas the differences increase for E_2 and ν_{21} for higher values of θ. The values of E_1 and ν_{12} are much controlled than the classical case as the values increase rapidly for lower values of θ for the classical case. It is noticed that the effect of β on the material parameters is significant and the lattice become more flexible as the β takes a higher value. This tells us that a more flexible lattice can be obtained by introducing a curved beam and can exploit flexibility for a particular value of θ wherever needed. By varying the curvature angle β value the material properties can be tuned to the extent which is not possible within the scope of classical straight-beam lattices.

To get an overall vision of how the material parameters are getting influenced by the crucial latices parameters, a 3D plot is shown in

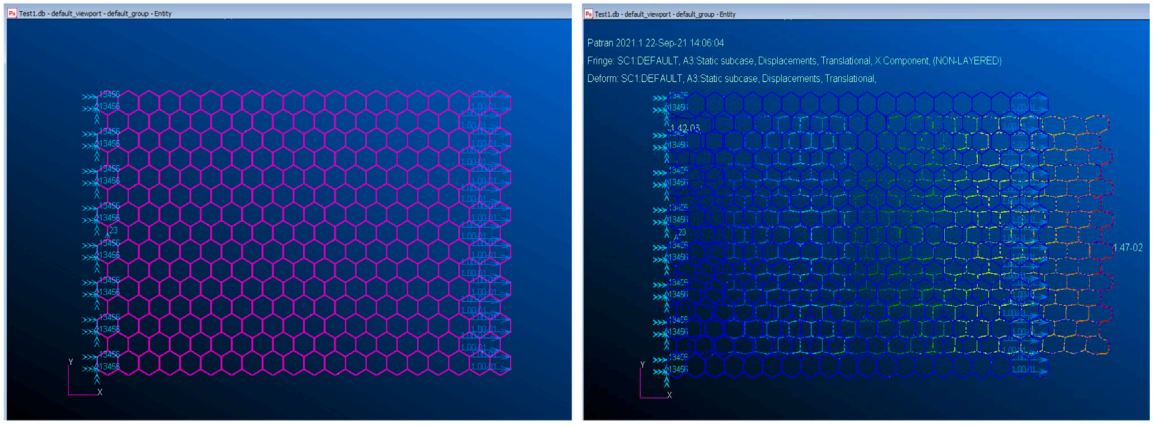

(a) Finite element model (b) Deformed shape

Fig. 9. Figure showing (a) Finite element model of the entire lattice with boundary conditions (fixed left side, uniformly distributed load is the right side) (b) deformed shape of the lattice due to the application of load in the x-direction.

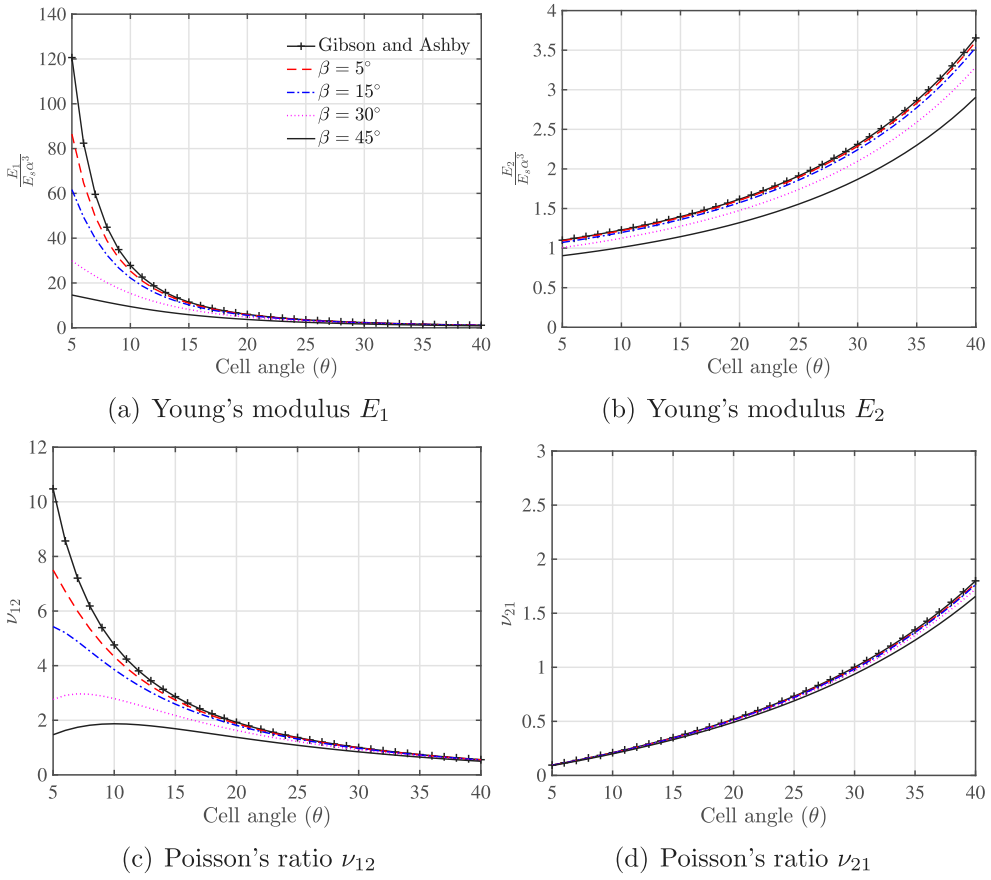

(a) Young's modulus E_1 (b) Young's modulus E_2

(c) Poisson's ratio ν_{12} (d) Poisson's ratio ν_{21}

Fig. 10. Comparison of normalised equivalent elastic moduli and Poisson's ratio obtained for curved hexagonal lattices and regular hexagonal lattices considering Gibson and Ashby's formula. The results are plotted as functions of cell angle θ for a value of height ratio $\eta = \frac{h}{L} = 1$ and different values of curvature angle (β).

Fig. 11. This describes the nature of the variability of the equivalent elastic properties of the lattices as functions of the cell angle θ and the curvature angle β.

Later we will see that when the axial deformations are included, the values of the equivalent elastic moduli and Poisson's ratio of the lattice are reduced and the lattice system will become more flexible for the curved geometry. This shows the larger design space of the curved lattices in comparison to the straight lattice. In the case of the curved lattice, there is one additional parameter, the curvature angle (β) and combinations of θ, β and η can be utilised to tune the equivalent properties as per the design requirements.

6. Generalisation to further geometries and special cases

In Section 3, we obtained the analytical expressions for the Young's modulus and Poisson's ratios (Eqs. (43), (45), (51) and (52)) for the curved hexagonal lattice. The formulation is very general and it can be applied to various other lattice patterns and geometry of the constituent members. Seven special cases of various patterns which include curved

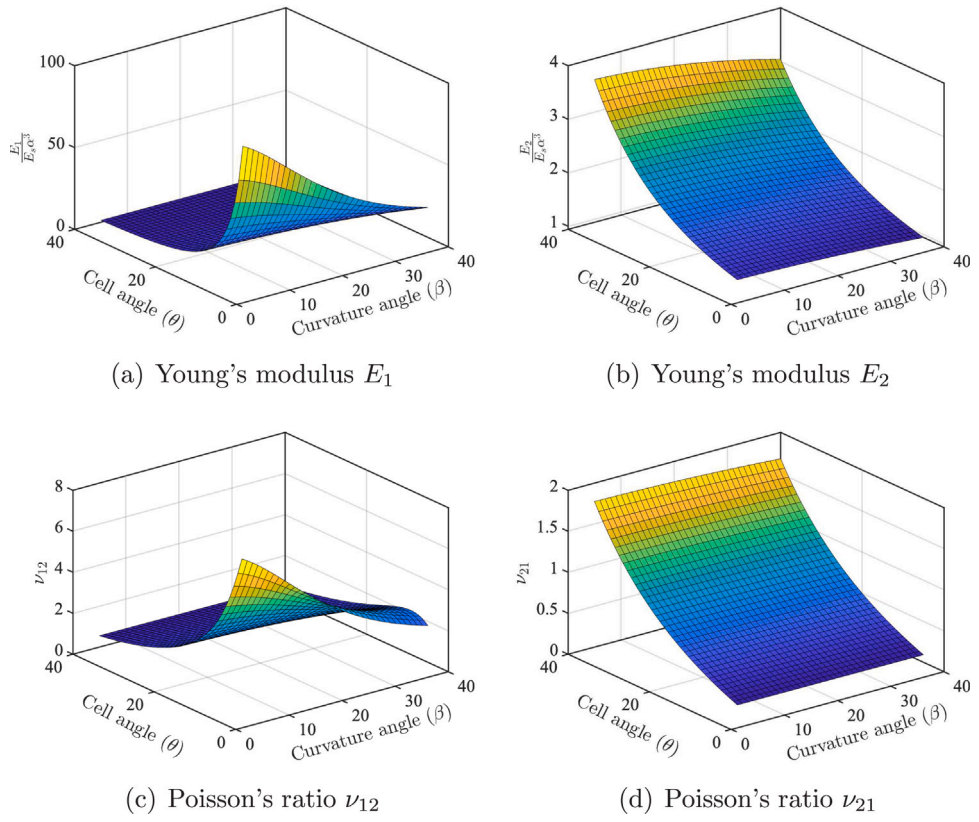

Fig. 11. Normalised equivalent elastic moduli and Poisson's ratio obtained for hexagonal curved lattice; The results are plotted as functions of cell angle θ and curvature angle β for a value of height ratio $\eta = \frac{h}{L} = 1$.

auxetic hexagonal lattice ($\theta = -\theta$), curved rhombus lattice ($h = 0$), curved rectangular lattice ($\theta = 0$), regular hexagonal lattice ($\beta = 0$), regular auxetic hexagonal lattice ($\theta = -\theta, \beta = 0$), regular rhombus lattice ($h = 0, \beta = 0$), and regular rectangular lattice ($\theta = 0, \beta = 0$) are shown in Fig. 12.

The unit cells for those lattices are also highlighted in Fig. 12. In this section, we derive and discuss the equivalent in-plane elastic moduli and Poisson's ratios for all these cases considering the general expressions Eqs. (43), (45), (51) and (52) in separate subsections.

6.1. The curved auxetic hexagonal lattice: $\beta \neq 0, \theta = -\theta$ and $\eta \neq 0$

This is a novel class of re-entrant lattice introduced in this paper. The schematic diagram of the lattice is shown Fig. 12(b). A more realistic 3D representation of this lattice can be seen in Fig. 1(b). The expressions for the equivalent elastic moduli and Poisson's ratios are obtained from the expressions of curved hexagonal lattice derived in Section 3 considering $\theta = -\theta$. The explicit expressions of the equivalent elastic properties are given by

$$\begin{aligned} E_1 = \frac{\sigma_1}{\epsilon_1} &= \frac{\Delta \cos\theta}{b(\eta - \sin\theta)\left[k_{11}\sin^2\theta' + k_{22}\cos^2\theta' + k_{12}\sin\ 2\theta'\right]} \\ &= \frac{D_L \bar{\Delta}\cos\theta}{b(\eta - \sin\theta)\left[\bar{k}_{11}\sin^2\theta' + \bar{k}_{22}\cos^2\theta' + \bar{k}_{12}\sin\ 2\theta'\right]} \\ &= \frac{2}{3}E\alpha^3 \frac{\bar{\Delta}\cos\theta}{(\eta - \sin\theta)\left[\bar{k}_{11}\sin^2\theta' + \bar{k}_{22}\cos^2\theta' + \bar{k}_{12}\sin\ 2\theta'\right]} \end{aligned} \tag{58}$$

$$\nu_{12} = -\frac{\epsilon_2}{\epsilon_1} = \frac{\cos\theta}{(\eta - \sin\theta)} \frac{\left[\bar{k}_{12}\cos 2\theta' + 0.5(\bar{k}_{11} - \bar{k}_{22})\sin 2\theta'\right]}{\left[\bar{k}_{11}\sin^2\theta' + \bar{k}_{22}\cos^2\theta' + \bar{k}_{12}\sin\ 2\theta'\right]} \tag{59}$$

$$\begin{aligned} E_2 = \frac{\sigma_2}{\epsilon_2} &= \frac{\Delta(\eta - \sin\theta)}{b\left[(k_{11}\cos^2\theta' + k_{22}\sin^2\theta' - k_{12}\sin\ 2\theta') - \frac{2\Delta}{K_{44}^h}\right]\cos\theta} \\ &= \frac{2}{3}E\alpha^3 \frac{\bar{\Delta}(\eta - \sin\theta)}{\left[(\bar{k}_{11}\cos^2\theta' + \bar{k}_{22}\sin^2\theta' - \bar{k}_{12}\sin\ 2\theta') - \frac{4}{3}\eta\alpha^2\right]\cos\theta} \end{aligned} \tag{60}$$

and

$$\nu_{21} = -\frac{\epsilon_1}{\epsilon_2} = \frac{(\eta - \sin\theta)(\bar{k}_{12}\cos 2\theta' + 0.5(\bar{k}_{11} - \bar{k}_{22})\sin 2\theta')}{\left[(\bar{k}_{11}\cos^2\theta' + \bar{k}_{22}\sin^2\theta' - \bar{k}_{12}\sin\ 2\theta') - \frac{4}{3}\eta\alpha^2\right]\cos\theta} \tag{61}$$

For the auxetic lattice, we consider $\theta = \beta = \frac{\pi}{6}$ and $\eta = 2$ to perform the numerical calculations.

Fig. 13 shows the equivalent elastic moduli and Poisson's ratios as a function of cell angle (θ) for different values of curvature angle (β). In this plot, we compare our results with the classical Gibson and Ashby's case and also observed β has a significant effect on the flexibility of the structure for the lower value of θ for E_1 and ν_{12}. Whereas, for E_2 and ν_{21} the influence is not that much and the difference increases for higher θ values. By varying the β value the flexibility can be exploited as per the design requirements. We can play with the negative ν_{12} by varying the β. Fig. 14 reveals how the equivalent material parameters are varying with θ and β. From Fig. 15 we can observe that the β has a significant effect on values of E_1, E_2 and ν_{12}.

For a particular value of η, the value of E_1 for the auxetic lattice is higher than the regular lattice. Whereas, it is reverse for the E_2. In general, the flexibility is much higher for the curved lattices than the classical ones. The values of the Poisson's ratio ν_{12} is also controlled in comparison with the classical auxetic case. Also, the flexibility and Poisson's ratio can be adjusted as per our requirements for the auxetic curved lattice. The analytical expressions are used here to obtain these plots.

6.2. The curved rhombus lattice: $\beta \neq 0, \theta \neq 0$ and $\eta = 0$

The schematic diagram of this novel class of the lattice is shown Fig. 12(c) along with the shape of the unit cell used for the analysis. A

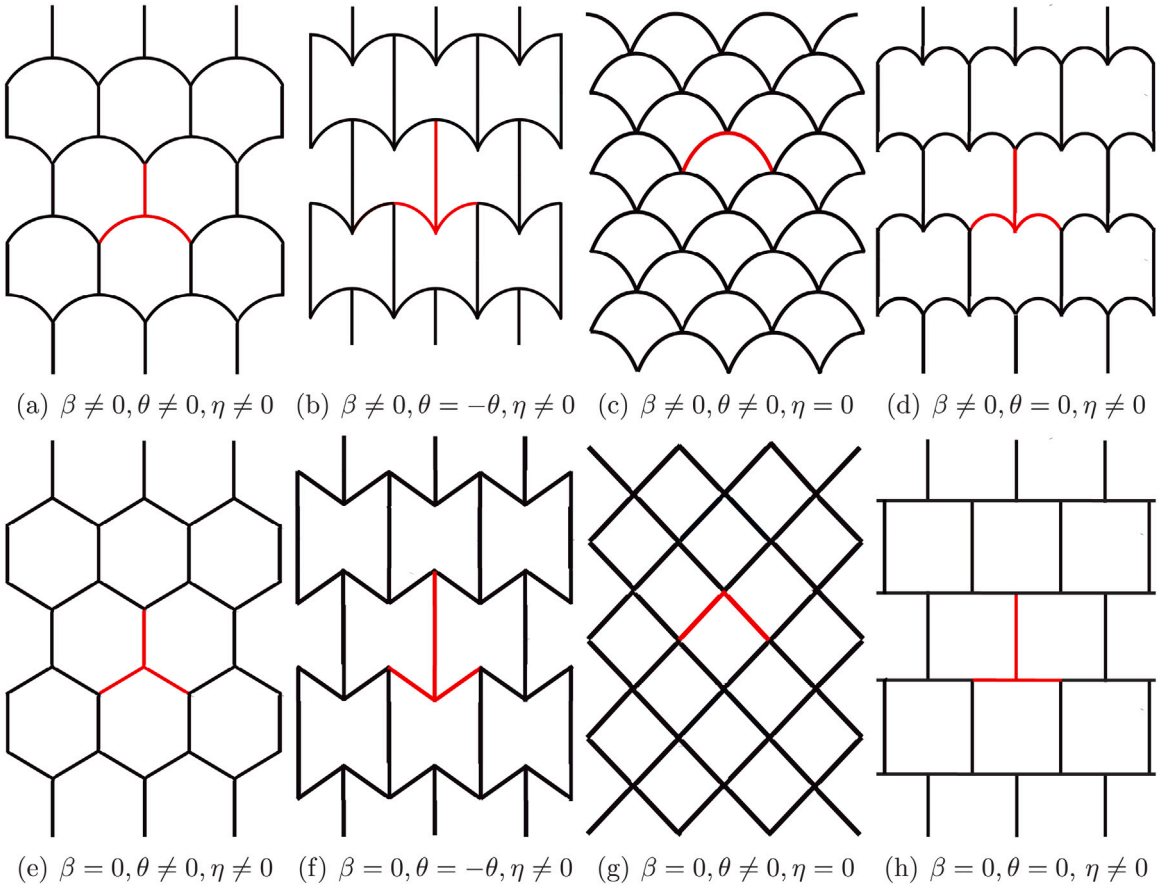

Fig. 12. Geometry of various lattices and corresponding unit cells. The family of lattices is created by considering special values of the cell angle (θ), curvature angle (β) and height ratio (η). The specific lattices are (a) curved hexagonal lattice ($\beta \neq 0, \theta \neq 0, \eta \neq 0$), (b) curved auxetic hexagonal lattice ($\beta \neq 0, \theta = -\theta, \eta \neq 0$), (c) curved rhombus lattice ($\beta \neq 0, \theta \neq 0, \eta = 0$), (d) curved rectangular lattice ($\beta \neq 0, \theta = 0, \eta \neq 0$), (e) regular hexagonal lattice ($\beta = 0, \theta \neq 0, \eta \neq 0$), (f) regular auxetic hexagonal lattice ($\beta = 0, \theta = -\theta, \eta \neq 0$), (g) regular rhombus lattice ($\beta = 0, \theta \neq 0, \eta = 0$), (h) regular rectangular lattice ($\beta = 0, \theta = 0, \eta \neq 0$). The special cases of straight lattices (e - h) are obtained from the corresponding curved hexagonal lattice (a - d) when $\beta = 0$.

3D representation of this lattice can be seen in Fig. 1(c). In this special case, the vertical straight beam is not present. This results in a lattice material consisting of only curved beam elements. This lattice is called a 'rhombus lattice' because its straight counterpart (in Fig. 12(g)) has rhombus-shaped unit cells.

The expressions for the equivalent Young's modulus and Poisson's ratios are obtained from the general curved lattice considering $\eta = \frac{h}{L} = 0$. After some simplifications, the equivalent elastic properties are expressed by the following closed-form expressions

$$\begin{aligned} E_1 = \frac{\sigma_1}{\epsilon_1} &= \frac{\Delta \cos\theta}{b \sin\theta \left[k_{11} \sin^2\theta' + k_{22} \cos^2\theta' + k_{12} \sin\ 2\theta'\right]} \\ &= \frac{D_L \bar{\Delta} \cos\theta}{b \sin\theta \left[\bar{k}_{11} \sin^2\theta' + \bar{k}_{22} \cos^2\theta' + \bar{k}_{12} \sin\ 2\theta'\right]} \\ &= \frac{2}{3} E \alpha^3 \frac{\bar{\Delta} \cos\theta}{\sin\theta \left[\bar{k}_{11} \sin^2\theta' + \bar{k}_{22} \cos^2\theta' + \bar{k}_{12} \sin\ 2\theta'\right]} \end{aligned} \tag{62}$$

$$\nu_{12} = -\frac{\epsilon_2}{\epsilon_1} = \frac{\cos\theta}{\sin\theta} \frac{\left[\bar{k}_{12} \cos 2\theta' + 0.5(\bar{k}_{11} - \bar{k}_{22}) \sin 2\theta'\right]}{\left[\bar{k}_{11} \sin^2\theta' + \bar{k}_{22} \cos^2\theta' + \bar{k}_{12} \sin\ 2\theta'\right]} \tag{63}$$

$$\begin{aligned} E_2 = \frac{\sigma_2}{\epsilon_2} &= \frac{\Delta \sin\theta}{b \left[(k_{11} \cos^2\theta' + k_{22} \sin^2\theta' - k_{12} \sin\ 2\theta') - \frac{2\Delta}{K^h_{44}}\right] \cos\theta} \\ &= \frac{2}{3} E \alpha^3 \frac{\bar{\Delta} \sin\theta}{\left[(\bar{k}_{11} \cos^2\theta' + \bar{k}_{22} \sin^2\theta' - \bar{k}_{12} \sin\ 2\theta') - \frac{4}{3}\eta\alpha^2\right] \cos\theta} \end{aligned} \tag{64}$$

and

$$\nu_{21} = -\frac{\epsilon_1}{\epsilon_2} = \frac{\sin\theta(\bar{k}_{12} \cos 2\theta' + 0.5(\bar{k}_{11} - \bar{k}_{22}) \sin 2\theta')}{\left[(\bar{k}_{11} \cos^2\theta' + \bar{k}_{22} \sin^2\theta' - \bar{k}_{12} \sin\ 2\theta') - \frac{4}{3}\eta\alpha^2\right] \cos\theta} \tag{65}$$

In the next subsection, we explore another geometry for curved lattice considering cell angle $\theta = 0$.

6.3. The curved rectangular lattice: $\beta \neq 0, \theta = 0$ and $\eta \neq 0$

This is another class of novel lattice with curved elements proposed in the paper. The schematic diagram of this lattice is shown Fig. 12(d) along with the shape of the unit cell used for the analysis. A more realistic 3D representation of this lattice can be seen in Fig. 1(d). In this special case, the inclined beams in the unit cell become horizontal as the cell angle $\theta = 0$. This lattice is called a 'rectangular lattice' because its straight counterpart (in Fig. 12(h)) has rectangular shaped unit cells.

The expressions for the equivalent Young's modulus and Poisson's ratios are obtained from the general curved lattice considering $\theta = 0$. After some simplifications, the equivalent elastic properties are expressed by the following closed-form expressions

$$\begin{aligned} E_1 &= \frac{\Delta}{b\eta \left[k_{11} \sin^2\beta + k_{22} \cos^2\beta + k_{12} \sin\ 2\beta\right]} \\ &= \frac{2}{3} E \alpha^3 \frac{\bar{\Delta}}{\sin\beta \left[\bar{k}_{11} \sin^2\theta + \bar{k}_{22} \cos^2\beta + \bar{k}_{12} \sin\ 2\beta\right]} \end{aligned} \tag{66}$$

$$\nu_{12} = \frac{\left[\bar{k}_{12} \cos 2\beta + 0.5(\bar{k}_{11} - \bar{k}_{22}) \sin 2\beta\right]}{\eta \left[\bar{k}_{11} \sin^2\beta + \bar{k}_{22} \cos^2\beta + \bar{k}_{12} \sin\ 2\beta\right]} \tag{67}$$

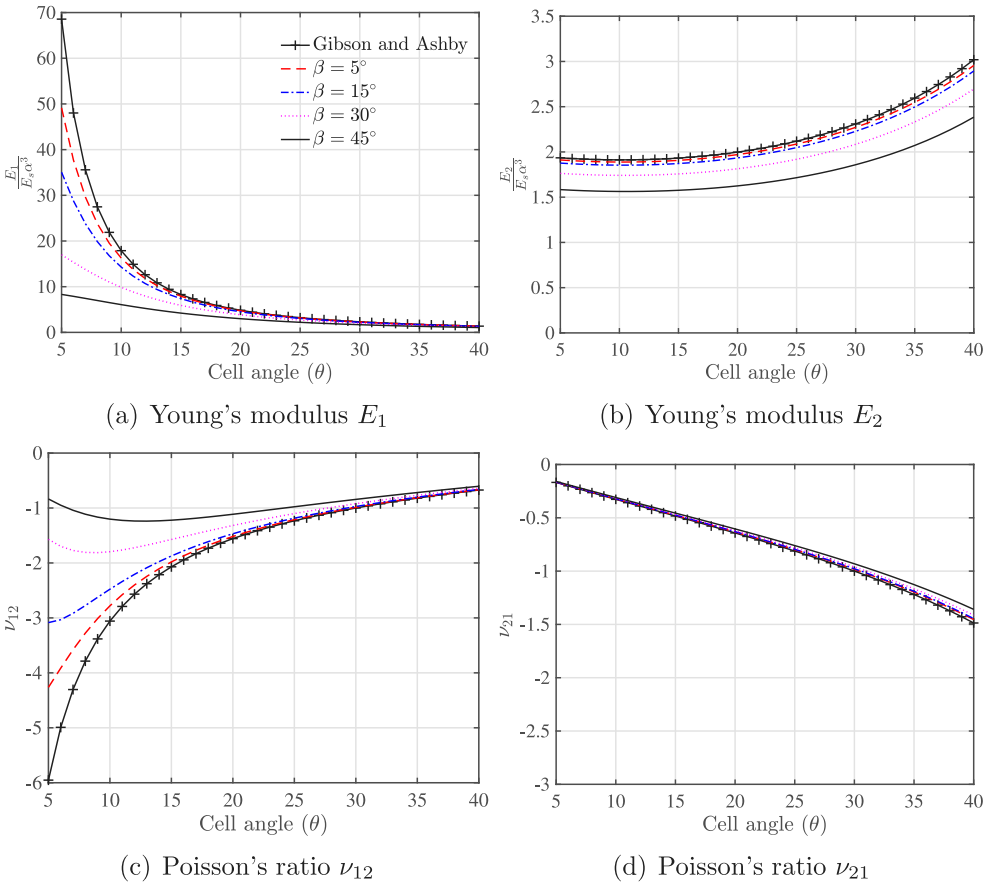

(a) Young's modulus E_1 (b) Young's modulus E_2

(c) Poisson's ratio ν_{12} (d) Poisson's ratio ν_{21}

Fig. 13. Comparison of normalised equivalent elastic moduli and Poisson's ratios obtained for curved auxetic hexagonal lattice and regular hexagonal lattice. The results are plotted as functions of cell angle θ for a value of height ratio $\eta = \frac{h}{L} = 2$ and different values of curvature angle (β).

$$E_2 = \frac{\Delta\eta}{b\left[(k_{11}\cos^2\beta + k_{22}\sin^2\beta - k_{12}\sin\ 2\beta) - \frac{2\Delta}{K_{44}^h}\right]} = \frac{2}{3}E\alpha^3\frac{\bar{\Delta}\eta}{\left[(\bar{k}_{11}\cos^2\beta + \bar{k}_{22}\sin^2\beta - \bar{k}_{12}\sin\ 2\beta) - \frac{4}{3}\eta\alpha^2\right]} \tag{68}$$

$$\text{and} \quad \nu_{21} = \frac{\eta(\bar{k}_{12}\cos 2\beta + 0.5(\bar{k}_{11} - \bar{k}_{22})\sin 2\beta)}{\left[(\bar{k}_{11}\cos^2\beta + \bar{k}_{22}\sin^2\beta - \bar{k}_{12}\sin\ 2\beta) - \frac{4}{3}\eta\alpha^2\right]} \tag{69}$$

The next subsections deal with the regular cases corresponding to their curved cases described before. In the next lattice, generalised expressions for the regular hexagonal lattice are derived.

6.4. *The regular hexagonal lattice:* $\beta = 0, \theta \neq 0$ *and* $\eta \neq 0$

The regular hexagonal lattice often referred to as the honeycomb, is the classical 2D lattice as shown in Fig. 12(e). This has been extensively investigated in literature and the equivalent elastic properties are given in Gibson and Ashby [4]. Here we explicitly demonstrate the classical one as a special case of the general expressions of the curved lattices derived here.

The expressions of the equivalent Young's modulus and Poisson's ratios for the regular hexagonal lattice can be obtained considering $\lim_{\beta\to 0}$ to the expressions of curved hexagonal lattice (Section 3; (Eqs. (43), (45), (51) and (52))). The resulting expressions are obtained as below

$$E_1 = \lim_{\beta\to 0}\frac{\Delta\cos\theta}{b(\eta + \sin\theta)\left[k_{11}\sin^2\theta' + k_{22}\cos^2\theta' + k_{12}\sin\ 2\theta'\right]} \tag{70}$$

The limiting values of the stiffness terms of the curved beam are the stiffness terms of the Euler–Bernoulli beam as shown in Eq. . For the sake of clarity let us consider the stiffness terms and explicitly take the limit $\lim_{\beta\to 0}$

$$k_{11}^{EB} = \lim_{\beta\to 0}k_{11} = \lim_{\beta\to 0}D\left[\beta^2 - \beta\left(\cos^2\beta - \sin^2\beta\right)\sin\beta\cos\beta - \frac{2}{1+\xi}\sin^4\beta\right] = \frac{EA}{L} \tag{71}$$

$$k_{22}^{EB} = \lim_{\beta\to 0}k_{22} = \lim_{\beta\to 0}D\left[\beta^2 + \beta\left(\cos^2\beta - \sin^2\beta\right)\sin\beta\cos\beta - \frac{2}{1+\xi}\sin^2\beta\cos^2\beta\right] = \frac{12EI}{L^3} \tag{72}$$

$$k_{12}^{EB} = \lim_{\beta\to 0}k_{12} = \lim_{\beta\to 0}D\left[2\beta\sin^2\beta\cos^2\beta - \frac{2}{1+\xi}\sin^3\beta\cos\beta\right] = 0 \tag{73}$$

$$\lim_{\beta\to 0}\Delta = \lim_{\beta\to 0}\left[k_{11}k_{22} - k_{12}^2\right] = \frac{12E^2IA}{L^4} \tag{74}$$

$$\text{and} \quad \lim_{\beta\to 0}\theta' = \lim_{\beta\to 0}(\theta + \beta) = \theta \tag{75}$$

Considering the limits and performing some algebraic operations we get the equivalent elastic properties as

$$E_1 = \frac{12E^2AI\cos\theta}{bL^4(\eta + \sin\theta)\left[\sin^2\theta\frac{EA}{L} + \frac{12EI}{L^3}\cos^2\theta\right]} = \frac{\frac{12EI}{L^3}\cos\theta}{b(\eta + \sin\theta)\left[\sin^2\theta + \frac{\frac{12EI}{L^3}}{\frac{EA}{L}}\cos^2\theta\right]}$$

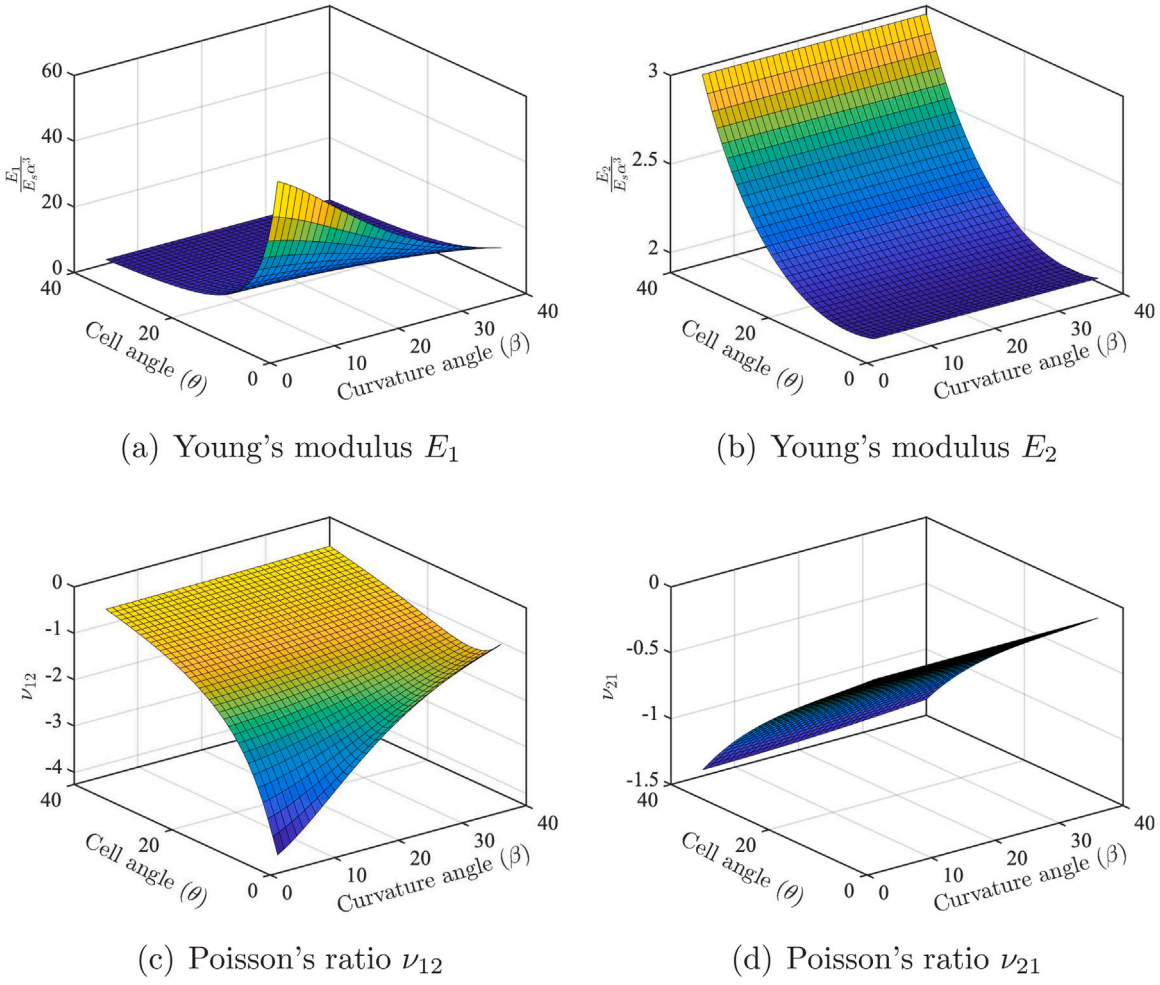

Fig. 14. Normalised equivalent elastic moduli and Poisson's ratios obtained for auxetic hexagonal curved lattice. The results are plotted as functions of cell angle θ and curvature angle β for a value of height ratio $\eta = \frac{h}{L} = 2$.

$$= \frac{k_{22}^{EB}\cos\theta}{b(\eta+\sin\theta)\left[\sin^2\theta + \frac{k_{22}^{EB}}{k_{11}^{EB}}\cos^2\theta\right]} = \frac{E\alpha^3\cos\theta}{(\eta+\sin\theta)\left(\sin^2\theta+\alpha^2\cos^2\theta\right)} \tag{76}$$

$$\begin{aligned} E_2 &= \lim_{\beta\to 0}\frac{\Delta(\eta+\sin\theta)}{b\left[(k_{11}\cos^2\theta' + k_{22}\sin^2\theta' - k_{12}\sin\ 2\theta') - \frac{2\Delta}{K_{44}^h}\right]\cos\theta} \\ &= \frac{k_{22}^{EB}(\eta+\sin\theta)}{b\cos\theta^3\left[1+\tan^2\theta\frac{k_{22}^{EB}}{k_{11}^{EB}} + 2\sec^2\theta\frac{k_{22}^{EB}}{k_{11}^{EBh}}\right]} \\ &= \frac{E\alpha^3(\eta+\sin\theta)}{(1-\alpha^2)\cos^3\theta\ +\alpha^2(2\eta+1)\cos\theta} \end{aligned} \tag{77}$$

$$\begin{aligned} \nu_{12} &= \lim_{\beta\to 0}\frac{\cos\theta}{(\eta+\sin\theta)}\frac{\left[k_{12}\cos 2\theta' + 0.5(k_{11}-k_{22})\sin 2\theta'\right]}{\left[k_{11}\sin^2\theta' + k_{22}\cos^2\theta' + k_{12}\sin\ 2\theta'\right]} \\ &= \frac{\cos^2\theta(1-\frac{k_{22}^{EB}}{k_{11}^{EB}})}{(\eta+\sin\theta)\sin\theta(1+\cot^2\theta\frac{k_{22}^{EB}}{k_{11}^{EB}})} = \frac{(1-\alpha^2)\cos^2\theta}{(\eta+\sin\theta)\sin\theta\left(1+\alpha^2\cot^2\theta\right)} \end{aligned} \tag{78}$$

and

$$\nu_{21} = \lim_{\beta\to 0}\frac{(\eta+\sin\theta)(k_{12}\cos 2\theta' + 0.5(k_{11}-k_{22})\sin 2\theta')}{\left[(k_{11}\cos^2\theta' + k_{22}\sin^2\theta' - k_{12}\sin\ 2\theta') - \frac{4}{3}\eta\alpha^2\right]\cos\theta}$$

$$= \frac{(\eta+\sin\theta)\sin\theta(1-\frac{k_{22}^{EB}}{k_{11}^{EB}})}{\left[1+\tan^2\theta\frac{k_{22}^{EB}}{k_{11}^{EB}} + 2\sec^2\theta\frac{k_{22}^{EB}}{k_{11}^{EBh}}\right]\cos^2\theta} = \frac{(1-\alpha^2)\sin\theta(\eta+\sin\theta)}{(1-\alpha^2)\cos^2\theta\ +\alpha^2(2\eta+1)} \tag{79}$$

The above expressions consider the axial compressing and stretching effect of the straight beams. This was ignored (assumed to be infinitely stiff) in the original expressions in Gibson and Ashby [4]. For a thin beam, the thickness ratio $\alpha \ll 1$. Using this in the above expressions (that is, substituting $\alpha^2 = 0$), it can be seen that they exactly reduce to the equivalent expressions in Gibson and Ashby [4] for a regular hexagonal lattice. This demonstrates the general nature of the analytical expressions derived here.

6.5. *The regular auxetic hexagonal lattice: $\beta = 0, \theta = -\theta$ and $\eta \neq 0$*

This is the conventional re-entrant lattice, as shown in Fig. 12(f). A key difference between a re-entrant (auxetic) hexagonal lattice and a regular hexagonal lattice discussed in the previous subsection is that the Poisson's ratios are negative valued for the auxetic lattice.

The expressions for the equivalent elastic properties of a regular auxetic hexagonal lattice are obtained by considering $\theta = -\theta$ and $\beta = 0$ to the expressions of general curved hexagonal lattice derived in Section 3. Performing these mathematical substitutions, the resulting

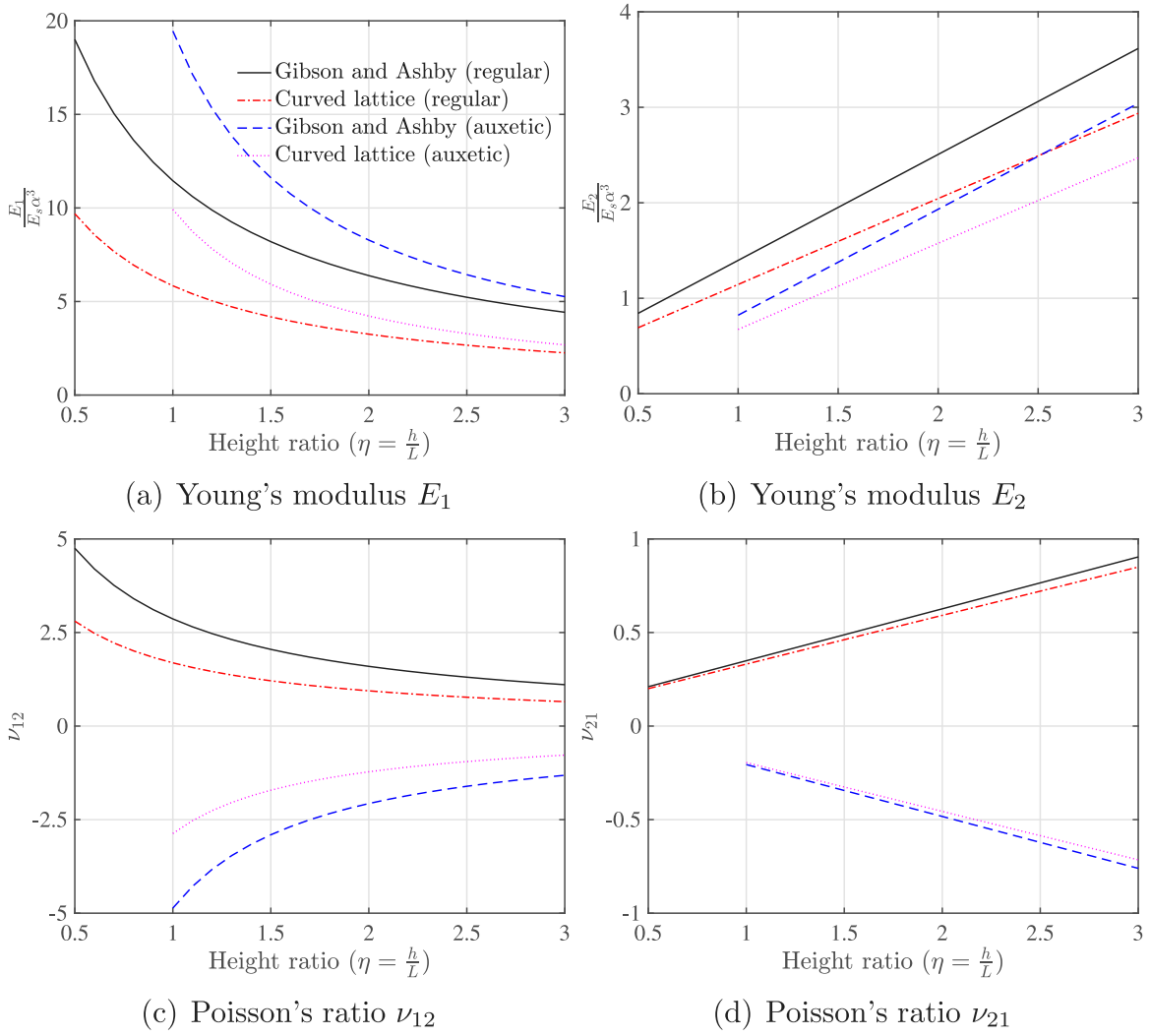

Fig. 15. Comparison of normalised equivalent elastic moduli and Poisson's ratios obtained for regular and auxetic case considering curved lattice and Gibson and Ashby formula. The results are plotted as function of height ratio $\eta = \frac{h}{L}$ for a value of cell angle $\theta = 15°$ and curvature angle $\beta = 45°$.

expressions are as follows

$$E_1 = \frac{k_{22}^{EB}\cos\theta}{b(\eta-\sin\theta)\left[\sin^2\theta + \frac{k_{22}^{EB}}{k_{11}^{EB}}\cos^2\theta\right]} = \frac{E\alpha^3\cos\theta}{(\eta-\sin\theta)\left(\sin^2\theta+\alpha^2\cos^2\theta\right)} \tag{80}$$

$$E_2 = \frac{k_{22}^{EB}(\eta-\sin\theta)}{b\cos^3\theta\left[1+\tan^2\theta\frac{k_{22}^{EB}}{k_{11}^{EB}} + 2\sec^2\theta\frac{k_{22}^{EB}}{k_{11}^{EBh}}\right]} = \frac{E\alpha^3(\eta-\sin\theta)}{(1-\alpha^2)\cos^3\theta\ +\alpha^2(2\eta+1)\cos\theta} \tag{81}$$

$$\nu_{12} = -\frac{\cos^2\theta(1-\frac{k_{22}^{EB}}{k_{11}^{EB}})}{(\eta-\sin\theta)\sin\theta(1+\cot^2\theta\frac{k_{22}^{EB}}{k_{11}^{EB}})} = -\frac{(1-\alpha^2)\cos^2\theta}{(\eta-\sin\theta)\sin\theta\left(1+\alpha^2\cot^2\theta\right)} \tag{82}$$

$$\text{and}\quad \nu_{21} = -\frac{(\eta-\sin\theta)\sin\theta(1-\frac{k_{22}^{EB}}{k_{11}^{EB}})}{\left[1+\tan^2\theta\frac{k_{22}^{EB}}{k_{11}^{EB}} + 2\sec^2\theta\frac{k_{22}^{EB}}{k_{11}^{EBh}}\right]\cos^2\theta} = -\frac{(1-\alpha^2)\sin\theta(\eta-\sin\theta)}{(1-\alpha^2)\cos^2\theta\ +\alpha^2(2\eta+1)} \tag{83}$$

Like the case of regular hexagonal lattice in the previous section, the classical expressions in Gibson and Ashby [4] are obtained by substituting $\alpha^2 = 0$ in these formulae. The next section deals with the regular rhombus lattice, obtained by considering the curvature angle $\beta = 0$.

6.6. *The regular rhombus lattice: $\beta = 0, \theta \neq 0$ and $\eta = 0$*

The rhombus lattice is obtained when $h = 0$ (that is $\eta = 0$). This implies the absence of the vertical member in the unit cell as shown in Fig. 12(g). The expressions of the equivalent elastic properties for the regular rhombus lattice are obtained considering $\lim_{\eta\to 0}$ to the expressions of curved hexagonal lattice derived in Section 3. The new expressions are given below as

$$E_1 = \lim_{\eta\to 0}\frac{12E^2AI\cos\theta}{bL^4(\eta+\sin\theta)\left[\sin^2\theta\frac{EA}{L} + \frac{12EI}{L^3}\cos^2\theta\right]} = \frac{k_{22}^{EB}\cos\theta}{b\sin\theta\left[\sin^2\theta + \frac{k_{22}^{EB}}{k_{11}^{EB}}\cos^2\theta\right]} = \frac{E\alpha^3}{\sin\theta\left(\sin^2\theta+\alpha^2\cos^2\theta\right)} \tag{84}$$

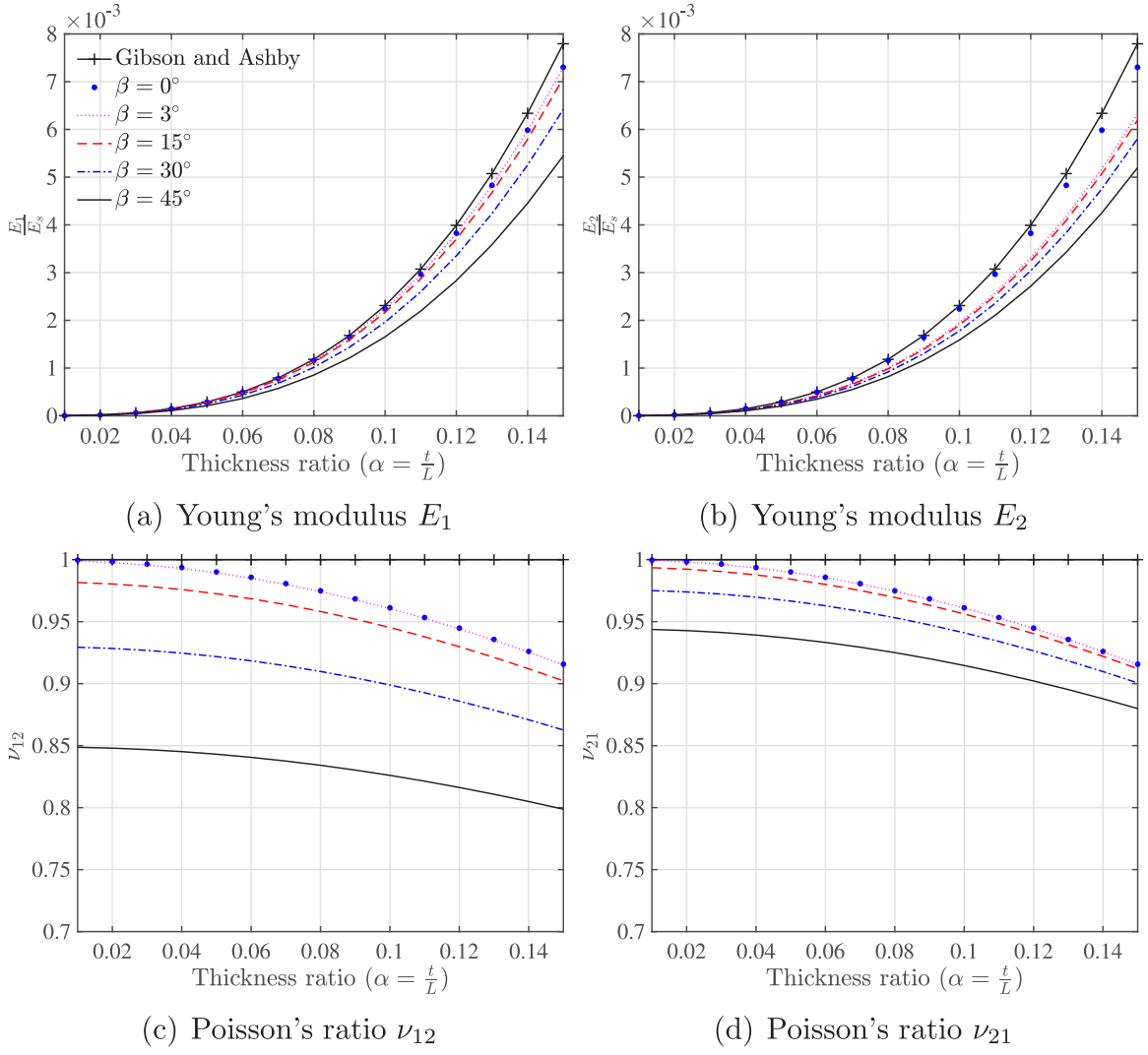

Fig. 16. Comparison of equivalent elastic moduli and Poisson's ratio obtained for curved hexagonal lattice and regular hexagonal lattice. The results are plotted as a function of thickness ratio $\alpha = \frac{t}{L}$ for cell angle $\theta = 30°$ and height ratio $\eta = \frac{h}{L} = 1$.

$$E_2 = \lim_{\eta\to 0} \frac{\Delta(\eta + \sin\theta)}{b\left[(k_{11}\cos^2\theta' + k_{22}\sin^2\theta' - k_{12}\sin\ 2\theta') - \frac{2\Delta}{K_{44}^h}\right]\cos\theta}$$
$$= \frac{k_{22}^{EB}\sin\theta}{b\cos^3\theta\left[1+\tan^2\theta\frac{k_{22}^{EB}}{k_{11}^{EB}}\right]} = \frac{E\alpha^3\sin\theta}{\cos\theta\left(\cos^2\theta+\alpha^2\sin^2\theta\right)} \tag{85}$$

$$\nu_{12} = \lim_{\eta\to 0}\frac{\cos\theta}{(\eta+\sin\theta)}\frac{\left[k_{12}\cos 2\theta' + 0.5(k_{11}-k_{22})\sin 2\theta'\right]}{\left[k_{11}\sin^2\theta' + k_{22}\cos^2\theta' + k_{12}\sin\ 2\theta'\right]}$$
$$= \frac{\cos^2\theta(1-\frac{k_{22}^{EB}}{k_{11}^{EB}})}{\sin^2\theta(1+\cot^2\theta\frac{k_{22}^{EB}}{k_{11}^{EB}})}$$
$$= \frac{\cos^2\theta(1-\alpha^2)}{\sin^2\theta(1+\alpha^2\cot^2\theta)} \tag{86}$$

and

$$\nu_{21} = \lim_{\eta\to 0}\frac{(\eta+\sin\theta)(k_{12}\cos 2\theta' + 0.5(k_{11}-k_{22})\sin 2\theta')}{\left[(k_{11}\cos^2\theta' + k_{22}\sin^2\theta' - k_{12}\sin\ 2\theta') - \frac{4}{3}\eta\alpha^2\right]\cos\theta}$$
$$= \frac{\sin^2\theta(1-\frac{k_{22}^{EB}}{k_{11}^{EB}})}{\left[1+\tan^2\theta\frac{k_{22}^{EB}}{k_{11}^{EB}}\right]\cos^2\theta} = \frac{\sin^2\theta(1-\alpha^2)}{\cos^2\theta\left(1+\alpha^2\tan^2\theta\right)} \tag{87}$$

The last subsection describes the regular rectangular lattice which is a special case of the curved rectangular lattice.

6.7. *The regular rectangular lattice: $\beta = 0, \theta = 0$ and $\eta \neq 0$*

The regular rectangular lattice is obtained when $\theta = \beta = 0$ and is shown in Fig. 12(h). The expressions of the equivalent elastic properties for the regular rectangular lattice are obtained considering $\lim_{\theta\to 0}$ to the expressions of curved hexagonal lattice Section 3.

$$E_1 = \lim_{\theta\to 0}\frac{k_{22}^{EB}\cos\theta}{b(\eta+\sin\theta)\left[\sin^2\theta + \frac{k_{22}^{EB}}{k_{11}^{EB}}\cos^2\theta\right]} = \frac{EA}{bh} = \frac{E\alpha}{\eta} \tag{88}$$

$$E_2 = \lim_{\theta\to 0}\frac{k_{22}^{EB}(\eta+\sin\theta)}{b\cos^3\theta\left[1+\tan^2\theta\frac{k_{22}^{EB}}{k_{11}^{EB}} + 2\sec^2\theta\frac{k_{22}^{EB}}{k_{11}^{EBh}}\right]} = \frac{E\alpha^3}{\left[1+2\eta\alpha^2\right]} \tag{89}$$

$$\nu_{12} = \lim_{\theta\to 0}\frac{\cos^2\theta(1-\frac{k_{22}^{EB}}{k_{11}^{EB}})}{(\eta-\sin\theta)\sin\theta(1+\cot^2\theta\frac{k_{22}^{EB}}{k_{11}^{EB}})} = 0 \tag{90}$$

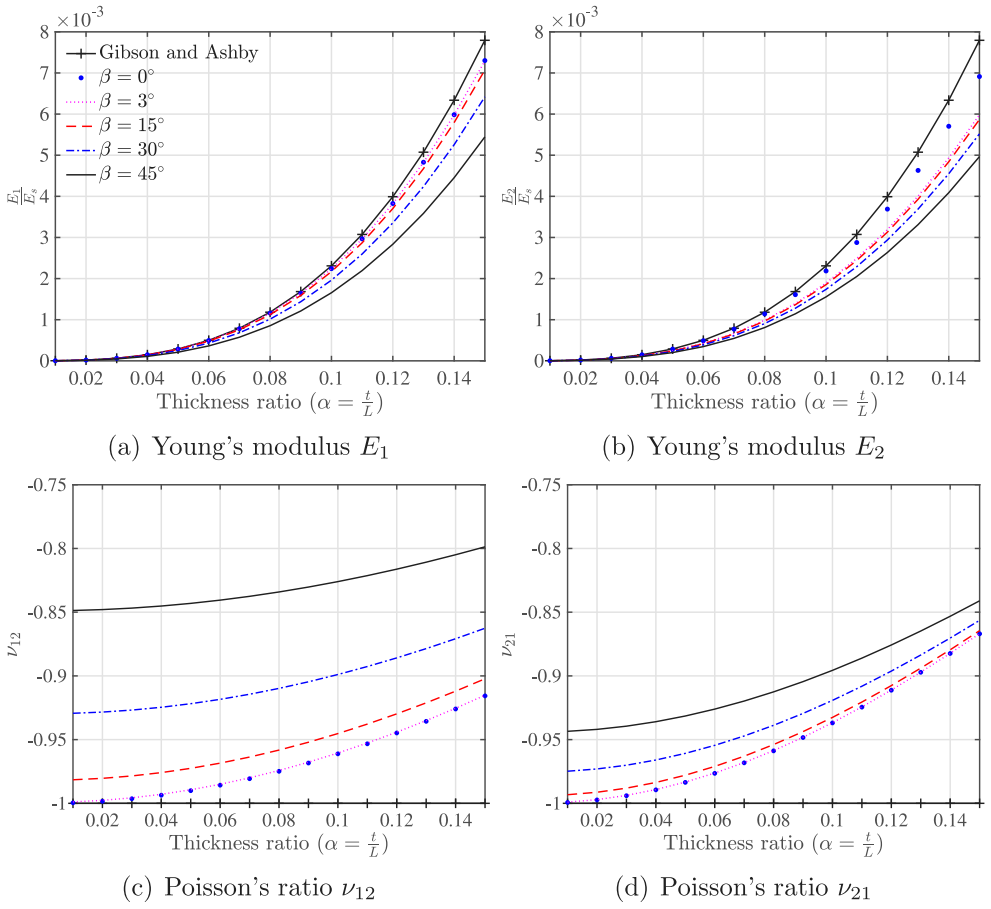

Fig. 17. Comparison of equivalent elastic moduli and Poisson's ratio obtained for curved auxetic hexagonal lattice and regular auxetic hexagonal lattice. The results are plotted as a function of thickness ratio $\alpha = \frac{t}{L}$ for cell angle $\theta = 30°$ and height ratio $\eta = \frac{h}{L} = 2$.

$$\text{and} \quad \nu_{21} = \lim_{\theta \to 0} \frac{(\eta + \sin\theta)\sin\theta(1 - \frac{k_{22}^{EB}}{k_{11}^{EB}})}{\left[1 + \tan^2\theta \frac{k_{22}^{EB}}{k_{11}^{EB}} + 2\sec^2\theta \frac{k_{22}^{EB}}{k_{11}^{EB^h}}\right]\cos^2\theta} = 0 \tag{91}$$

Note that both Poisson's ratios are zero for the regular rectangular lattice, which was not obvious for the case of the curved rectangular lattice discussed before. The following section deals with the numerical analysis considering the above mentioned curved geometries and their regular versions.

7. Numerical results: Comparison between two distinct group of lattices

A numerical comparison between two distinct groups of lattices mentioned in Fig. 12, namely the curved and the straight ones are conducted. Fig. 16 displays a comparison between the material properties obtained for the curved hexagonal and regular hexagonal lattice case.

The material properties are plotted as a function of thickness ratio ($\alpha = \frac{t}{L}$). The equivalent Young's moduli are normalised by Young's modulus of the Aluminum. The incorporation of a curved beam adds more flexibility to the lattice and as the β values go small the results from the curved case converge to the regular hexagonal case. For Poisson's ratios the effect of β is more for lower α values and we can control the E_1 and ν_{12} by varying the β value.

Curved auxetic and the regular auxetic cases are compared in Fig. 17.

Here also, we can make a similar observation like Fig. 16 that curved beam add more flexibility to the lattice and as the β values go small the results from the curved case converge to the regular hexagonal case and the effect of β is more for lower α values for Poisson's ratios.

Figs. 18 and 19 represent the comparison of the curved rhombus lattice (Fig. 12(c)) and its regular version (Fig. 12(g)) and curved rectangular (Fig. 12(d)) and regular rectangular version (Fig. 12(h)) respectively.

From the expressions of Young's modulus and Poisson's ratios for the special cases, the presence of a stretching term (Eq. (76)–(91)) can be observed. To visualise the effect of axial stretching and curved beam we plotted them and compare them with the classical Gibson and Ashby's [4] formula (Figs. 16–19). It is evident that the axial stretching has a significant effect on the flexibility of the material parameters and the flexibility can further be increased by incorporating curved beam elements as a constituent member of the unit cell. With the help of a curved beam element, we can tune the flexibility of the material by considering different values for the curvature angle (β) as per our requirements.

8. Conclusions

A novel class of 2D lattices comprised of curved elements is conceptualised, theoretically investigated and numerically validated in this paper. A bottom-up, general and rigorous analytical framework is developed to obtain closed-form expressions of Young's moduli and Poisson's ratios of such lattices and they are summarised in Fig. 20.

The developed generalised expressions are then utilised to obtain the equivalent elastic moduli and Poisson's ratios for several other physically realistic unique geometries. The usefulness of curved constituent elements in the unit cell to exploit the flexibility of the structure is

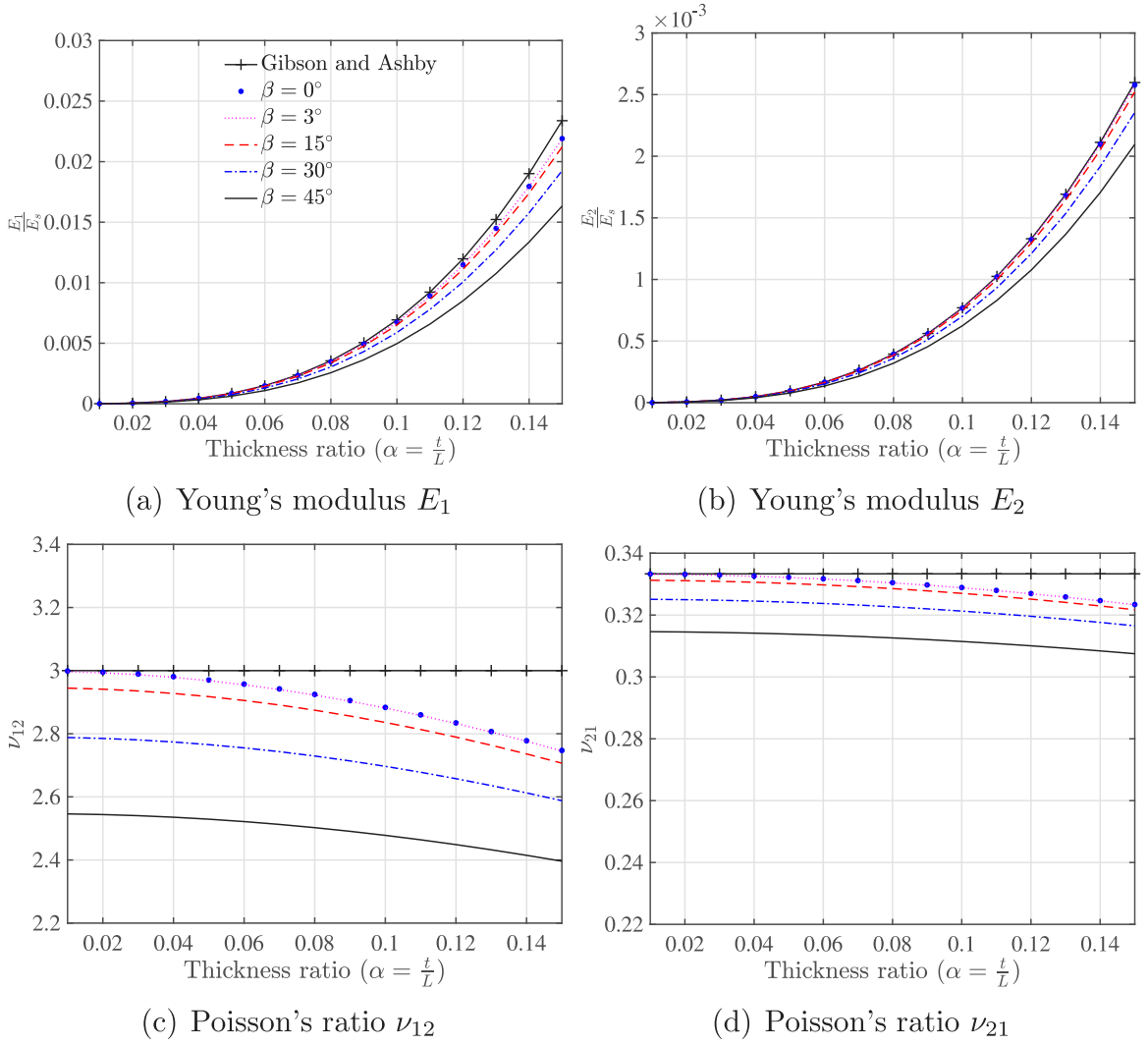

Fig. 18. Comparison of equivalent elastic moduli and Poisson's ratio obtained for curved rhombus lattice and regular rhombus lattice. The results are plotted as a function of thickness ratio $\alpha = \frac{t}{L}$ for cell angle $\theta = 30°$ and height ratio $\eta = \frac{h}{L} = 1$.

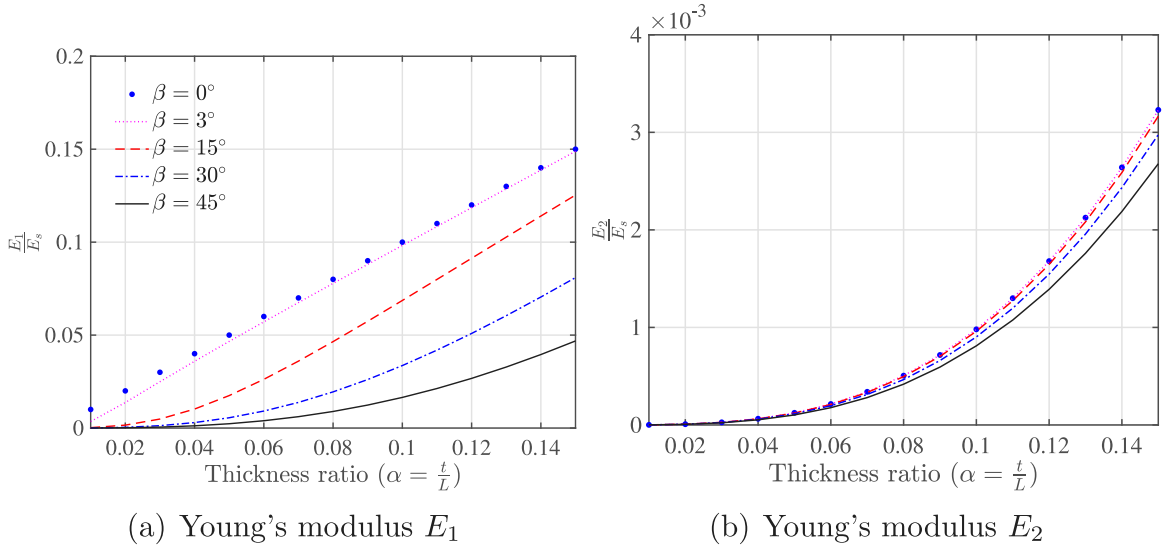

Fig. 19. Comparison of equivalent elastic moduli and Poisson's ratio obtained for curved rectangular lattice and regular rectangular lattice; The results are plotted as a function of thickness ratio $\alpha = \frac{t}{L}$ for cell angle $\theta = 30°$ and height ratio $\eta = \frac{h}{L} = 1$.

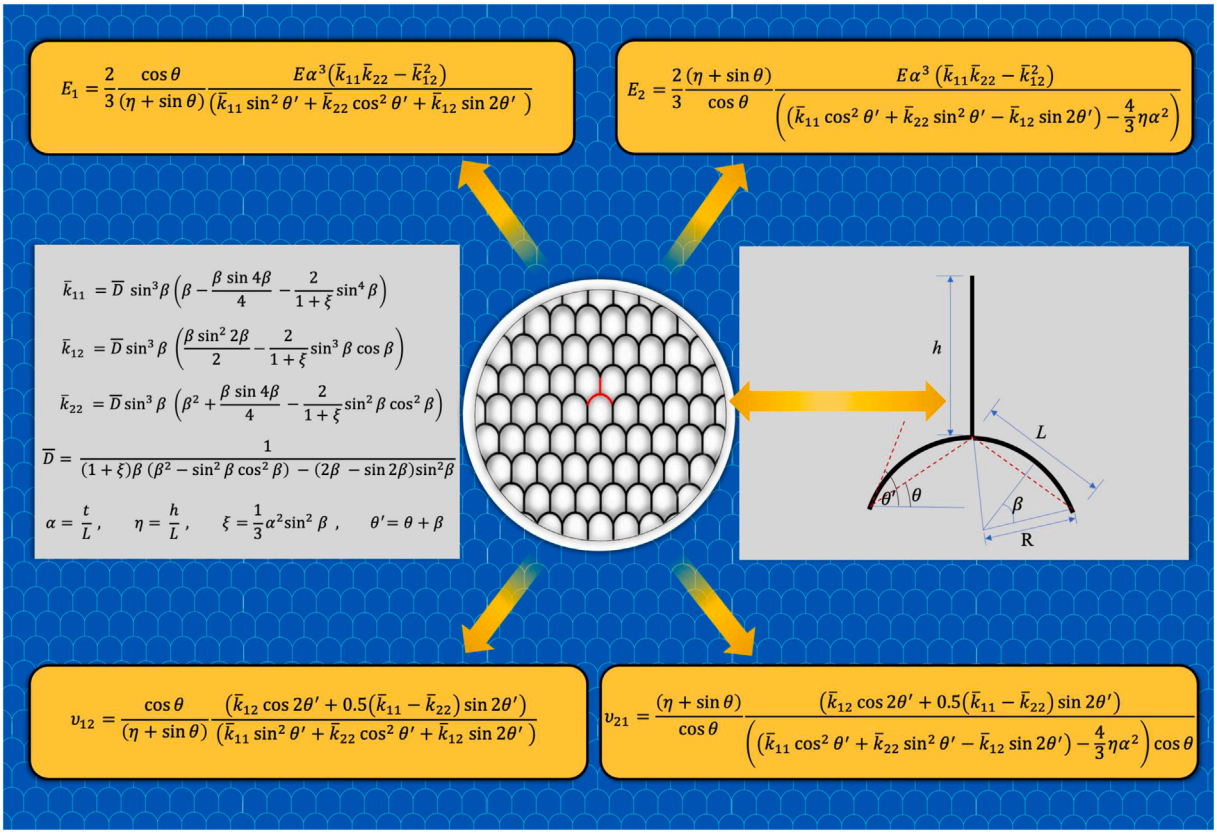

Fig. 20. Summary of the closed-form expressions of the equivalent in-plane elastic properties (E_1, E_2, ν_{12} and ν_{21}) of the novel hexagonal curved lattice introduced in the paper. The geometric parameters relevant to the equivalent elastic properties are shown in the unit cell diagram. The four parameters which completely control the elastic properties are: the thickness ratio $\alpha = t/L$, the height ratio $\eta = h/L$, the cell angle θ and the curvature angle β.

explored. The use of curved beams increases the design space compared to the lattices with straight constituent beam elements only. The curvature angle turns out to play an important role in altering and tailoring the equivalent elastic properties of these novel class of lattices. Unlike a conventional straight-beam lattice, the combined effect of the cell angle and the curvature angle can be utilised simultaneously in curved lattices. The combination of these two angles, along with the other geometric parameters such as thickness ratio and the height ratio give the widest possible family of 2D lattices to be considered in a unified manner. The proposed formulas incorporate the stretching effect of the individual members of the unit cell. It was explicitly shown that the expressions converge to the well-known classical formula for conventional hexagonal lattices as a special case. Major contributions to the state-of-the-art include:

- A new methodology to obtain closed-form expressions for equivalent in-plane elastic properties of hexagonal curved lattices using the coefficients of the stiffness matrix of constituent curved beams.
- The most general analytical expressions for equivalent elastic properties of 2D lattices, from which other geometries and special cases can be derived in a straightforward manner considering various mathematical limiting cases.
- The framework of an enriched design space and enhanced flexibility of the structure due to the inclusion of curved beam elements.
- The idea of the 'family of lattices', where different lattices appear physically distinct but are related to each other through a simple, and yet, a generalised underlying unified theoretical foundation.

The general analytical expressions of the equivalent elastic properties are exploited to study seven special cases of interest. They include, the curved auxetic hexagonal lattice, the curved rhombus lattice, the curved rectangular lattice, the regular hexagonal lattice, the regular auxetic hexagonal lattice, the regular rhombus lattice, and finally the regular rectangular lattice.

The expressions and the results obtained can be considered benchmark results for future research. It may be directly used for the design of flexible hexagonal lattices and other geometries. Future research directions will include exploring highly stretchable soft curved lattices with geometric nonlinearity and dynamic analysis.

CRediT authorship contribution statement

S. Mukherjee: Conceived the idea jointly, Generated the data and presented discussions of the results, Reviewed the manuscript, Critically examined the results, Checked the data and mathematical equations. **S. Adhikari:** Conceived the idea jointly, Conducted the literature review and contributed to the writing, Reviewed the manuscript, Critically examined the results, Checked the data and mathematical equations.

Declaration of competing interest

The authors declare that they have no known competing financial interests or personal relationships that could have appeared to influence the work reported in this paper.

References

[1] Park J, Wang S, Li M, Ahn C, Hyun JK, Kim DS, et al. Three-dimensional nanonetworks for giant stretchability in dielectrics and conductors. Nature Commun 2012;3(1):1–8.
[2] Schaedler TA, Carter WB. Architected cellular materials. Annu Rev Mater Res 2016;46:187–210.

[3] Frenzel T, Kadic M, Wegener M. Three-dimensional mechanical metamaterials with a twist. Science 2017;358(6366):1072–4.
[4] Gibson L, Ashby MF. Cellular solids structure and properties. Cambridge, UK: Cambridge University Press; 1999.
[5] Fleck NA, Deshpande VS, Ashby MF. Micro-architectured materials: past, present and future. Proc R Soc A 2010;466(2121):2495–516.
[6] Katz JL, Misra A, Spencer P, Wang Y, Bumrerraj S, Nomura T, Eppell SJ, Tabib-Azar M. Multiscale mechanics of hierarchical structure/property relationships in calcified tissues and tissue/material interfaces. Mater Sci Eng C 2007;27(3):450–68.
[7] Masters IG, Evans KE. Models for the elastic deformation of honeycombs. Compos Struct 1996;35(4):403–22.
[8] Abd El-Sayed F, Jones R, Burgess I. A theoretical approach to the deformation of honeycomb based composite materials. Composites 1979;10(4):209–14.
[9] Zschernack C, Wadee MA, Völlmecke C. Nonlinear buckling of fibre-reinforced unit cells of lattice materials. Compos Struct 2016;136:217–28.
[10] Balawi S, Abot J. A refined model for the effective in-plane elastic moduli of hexagonal honeycombs. Compos Struct 2008;84(2):147–58.
[11] Karakoç A, Santaoja K, Freund J. Simulation experiments on the effective in-plane compliance of the honeycomb materials. Compos Struct 2013;96:312–20.
[12] Harkati A, Bezazi A, Scarpa F, Ouisse M, et al. Out-of-plane elastic constants of curved cell walls honeycombs. Compos Struct 2021;268:113959.
[13] Veisi H, Farrokhabadi A. Investigation of the equivalent material properties and failure stress of the re-entrant composite lattice structures using an analytical model. Compos Struct 2021;257:113161.
[14] Adhikari S. The eigenbuckling analysis of hexagonal lattices: closed-form solutions. Proc R Soc Lond Ser A Math Phys Eng Sci 2021;477(2251):20210244.
[15] Mukherjee S, Adhikari S. A general analytical framework for the mechanics of heterogeneous hexagonal lattices. Thin-Walled Struct 2021;167:108188.
[16] Gibson L, Easterling K, Ashby MF. The structure and mechanics of cork. Proc R Soc Lond Ser A Math Phys Eng Sci 1981;377(1769):99–117.
[17] Mukhopadhyay T, Adhikari S. Effective in-plane elastic properties of auxetic honeycombs with spatial irregularity. Mech Mater 2016;95:204–22.
[18] Mukhopadhyay T, Adhikari S. Effective in-plane elastic moduli of quasi-random spatially irregular hexagonal lattices. Internat J Engrg Sci 2017;119:142–79.
[19] Adhikari S, Mukhopadhyay T, Shaw A, Lavery N. Apparent negative values of Young's moduli of lattice materials under dynamic conditions. Internat J Engrg Sci 2020;150:103231.
[20] Adhikari S, Mukhopadhyay T, Liu X. Broadband dynamic elastic moduli of honeycomb lattice materials: A generalized analytical approach. Mech Mater 2021;103796.
[21] Adhikari S. The in-plane mechanical properties of highly compressible and stretchable 2D lattices. Compos Struct 2021;272:114167.
[22] Malek S, Gibson L. Effective elastic properties of periodic hexagonal honeycombs. Mech Mater 2015;91:226–40.
[23] Huang T, Gong Y, Zhao S. Effective in-plane elastic modulus of a periodic regular hexagonal honeycomb core with thick walls. J Eng Mech 2018;144(2):06017019.
[24] Bornengo D, Scarpa F, Remillat C. Evaluation of hexagonal chiral structure for morphing airfoil concept. Proc Inst Mech Eng G 2005;219(3):185–92.
[25] Saito K, Agnese F, Scarpa F. A cellular kirigami morphing wingbox concept. J Intell Mater Syst Struct 2011;22(9):935–44.
[26] Bodaghi M, Damanpack A, Hu G, Liao W. Large deformations of soft metamaterials fabricated by 3D printing. Mater Des 2017;131:81–91.
[27] Weeger O, Boddeti N, Yeung S-K, Kaijima S, Dunn ML. Digital design and nonlinear simulation for additive manufacturing of soft lattice structures. Addit Manuf 2019;25:39–49.
[28] Jiang Y, Wang Q. Highly-stretchable 3D-architected mechanical metamaterials. Sci Rep 2016;6(1):1–11.
[29] Morin SA, Shepherd RF, Kwok SW, Stokes AA, Nemiroski A, Whitesides GM. Camouflage and display for soft machines. Science 2012;337(6096):828–32.
[30] Felton S, Tolley M, Demaine E, Rus D, Wood R. A method for building self-folding machines. Science 2014;345(6197):644–6.
[31] Restrepo D, Mankame ND, Zavattieri PD. Programmable materials based on periodic cellular solids. Part I: Experiments. Int J Solids Struct 2016;100:485–504.
[32] Yang H, Wang B, Ma L. Designing hierarchical metamaterials by topology analysis with tailored Poisson's ratio and Young's modulus. Compos Struct 2019;214:359–78.
[33] Baran T, Öztürk M. In-plane elasticity of a strengthened re-entrant honeycomb cell. Eur J Mech A Solids 2020;83:104037.
[34] Kang YJ, Yoo CH. Thin-walled curved beams. II: Analytical solutions for buckling of arches. J Eng Mech 1994;120(10):2102–25.
[35] Petyt M, Fleischer C. Free vibration of a curved beam. J Sound Vib 1971;18(1):17–30.
[36] Wu J-S, Chiang L-K. Free vibration analysis of arches using curved beam elements. Internat J Numer Methods Engrg 2003;58(13):1907–36.
[37] Yang F, Sedaghati R, Esmailzadeh E. Free in-plane vibration of general curved beams using finite element method. J Sound Vib 2008;318(4–5):850–67.
[38] Bogner F, Fox R, Schmit L. A cylindrical shell discrete element.. AIAA J 1967;5(4):745–50.
[39] Litewka P, Rakowski J. An efficient curved beam finite element. Internat J Numer Methods Engrg 1997;40(14):2629–52.
[40] Yang F, Sedaghati R, Esmailzadeh E. Free in-plane vibration of curved beam structures: a tutorial and the state of the art. J Vib Control 2018;24(12):2400–17.
[41] Eroglu U, Tufekci E. A new finite element formulation for free vibrations of planar curved beams. Mech Based Des Struct Mach 2018;46(6):730–50.
[42] Ashwell D, Sabir A. Limitations of certain curved finite elements when applied to arches. Int J Mech Sci 1971;13(2):133–9.
[43] Ashwell D, Sabir A, Roberts T. Further studies in the application of curved finite elements to circular arches. Int J Mech Sci 1971;13(6):507–17.
[44] Yamada Y, Ezawa Y. On curved finite elements for the analysis of circular arches. Internat J Numer Methods Engrg 1977;11(11):1635–51.
[45] Tufekci E, Eroglu U, Aya SA. A new two-noded curved beam finite element formulation based on exact solution. Eng Comput 2017;33(2):261–73.
[46] Su Y, Wang S, Huang Y, Luan H, Dong W, Fan JA, et al. Elasticity of fractal inspired interconnects. Small 2015;11(3):367–73.
[47] Ma Q, Cheng H, Jang K-I, Luan H, Hwang K-C, Rogers JA, et al. A nonlinear mechanics model of bio-inspired hierarchical lattice materials consisting of horseshoe microstructures. J Mech Phys Solids 2016;90:179–202.
[48] Liu J, Zhang Y. A mechanics model of soft network materials with periodic lattices of arbitrarily shaped filamentary microstructures for tunable poisson's ratios. J Appl Mech 2018;85(5).
[49] Liu J, Yan D, Zhang Y. Mechanics of unusual soft network materials with rotatable structural nodes. J Mech Phys Solids 2021;146:104210.
[50] Dawe D. Matrix and finite element displacement analysis of structures. Oxford, UK: Oxford University Press; 1984.
[51] Petyt M. Introduction to finite element vibration analysis. Cambridge, UK: Cambridge University Press; 1990.